Article

Human land use drives microplastic abundance in terrestrial wildlife

https://doi.org/10.1038/s41586-026-11285-x

Received: 9 July 2025

Accepted: 9 October 2026

Published online: 11 November 2026

Open access

Check for updates

Marcia de Almeida Monteiro Melo Ferraz[1,2,3]✉, Arnaud L. J. Desbiez[4,5], Mario Henrique Alves[4,6], Justin M. Calabrese[7,8,9,10], Alexandra Tiso Cumerlato[11], Fernanda Cristina Jacoby[11], Nicole Grechi[1], Danilo Kluyber[4,12], Erika Y. Lin[13], Marcella Pecora Milazzotto[14], Grazielle Soresini[4], Emília Patrícia Medici[11], Gabriela Mastromonaco[2] & Michael J. Noonan[3,15,16]

Plastic pollution is a defining feature of the Anthropocene[1], and microplastics are dispersed by air and water into even remote terrestrial habitats[2–7], yet the ecological and landscape-level processes that shape microplastic accumulation in terrestrial ecosystems remain poorly understood. Human land-use change is rapidly transforming landscapes worldwide, but the influence of this expanding human footprint on the microplastic burdens in wildlife remains largely unknown. This knowledge gap is particularly pressing in regions that are facing escalating environmental pressures, such as Brazil. Here we pair in vivo microplastic measurements with high-resolution tracking data from lowland tapirs and giant anteaters across Brazil and show that the microplastic burdens carried by free-ranging mammals increase with both the magnitude of their human footprint exposure and their proximity to development and waste management infrastructure. Microplastics were also detected in the blood of individuals occupying seemingly pristine habitats far from development, suggesting that direct exposure to human-modified landscapes is unlikely to be the sole driver of systemic microplastic burdens. In a period of accelerating global land-use change, these findings reveal how individual habitat use and anthropogenic land-use change interact to shape wildlife exposure to microplastics and suggest that managing animals' proximity to development and waste management infrastructure may reduce the microplastic burdens carried by terrestrial wildlife.

Plastic pollution, once thought to be a predominantly aquatic issue, is increasingly being recognized as a threat to terrestrial ecosystems[1]. Microplastics (synthetic polymer particles with diameter less than 5 mm) are a particularly problematic form of plastic pollution, as these small particles are easily dispersed through pathways that include atmospheric deposition, precipitation, river transport and groundwater flow[2–7]. The high environmental mobility of microplastics has allowed them to infiltrate even the most pristine habitats[8] where they can persist for centuries[9,10]. For wildlife exposed to microplastics, the small size and diverse chemistry of these particles facilitate ingestion[11] and the penetration of biological membranes[12,13]. Once internalized, microplastics can bioaccumulate, biomagnify through food webs and pose severe health risks[14–18].

Although much work has been done on detecting microplastics in different biological compartments (reviewed in ref. 19), studies in terrestrial ecosystems have largely been limited to descriptive surveys that document the presence of microplastics without investigating how these pollutants accumulate within wildlife[20–22]. Although such studies have proven informative for identifying the scope and scale of plastic pollution, this approach has left the bioaccumulation dynamics of microplastics in terrestrial environments poorly understood. As a result of this knowledge gap, even high-profile studies on plastic ingestion risk in wildlife have had to rely on assumptions about the relationship between individual habitat use and the uptake of microplastics rather than empirically grounded associations[23]. Because both sources and dispersal pathways for microplastics are amplified by land-use change[24–26], the intensity of human landscape modification should have a key role in shaping the internal microplastic burdens of terrestrial wildlife. Whether this is the case, however, is still largely unknown. With the continuing expansion of human-modified landscapes into wild spaces[27] and the concomitant increase in global plastic production[28], there is an urgent need to move beyond presence/absence studies and

[1]Gene Center, Ludwig-Maximilians-Universität München, Munich, Germany. [2]Reproductive Sciences Unit, Toronto Zoo, Toronto, Ontario, Canada. [3]Department of Biology, The University of British Columbia Okanagan, Kelowna, British Columbia, Canada. [4]Instituto de Conservação de Animais Silvestres (ICAS), Campo Grande, Brazil. [5]Royal Zoological Society of Scotland (RZSS), Edinburgh, UK. [6]Department of Veterinary Medicine, University of Bari, Valenzano, Bari, Italy. [7]Center for Advanced Systems Understanding (CASUS), Helmholtz-Zentrum Dresden-Rossendorf (HZDR), Görlitz, Germany. [8]Department of Geosciences, TUD Dresden University of Technology, Dresden, Germany. [9]Department of Ecological Modelling, Helmholtz Centre for Environmental Research-UFZ, Leipzig, Germany. [10]Department of Biology, University of Maryland, College Park, MD, USA. [11]Iniciativa Nacional para a Conservação da Anta Brasileira (INCAB), Instituto de Pesquisas Ecológicas (IPÊ), Campo Grande, Brazil. [12]Naples Zoo at Caribbean Gardens, Naples, FL, USA. [13]Department of Biology, University of Central Florida, Orlando, FL, USA. [14]Center of Natural and Human Sciences, Federal University of ABC, Santo André, Brazil. [15]Okanagan Institute for Biodiversity, Resilience, and Ecosystem Services, The University of British Columbia Okanagan, Kelowna, British Columbia, Canada. [16]Department of Math, Physics, and Statistics, The University of British Columbia Okanagan, Kelowna, British Columbia, Canada. ✉e-mail: m.ferraz@lmu.de

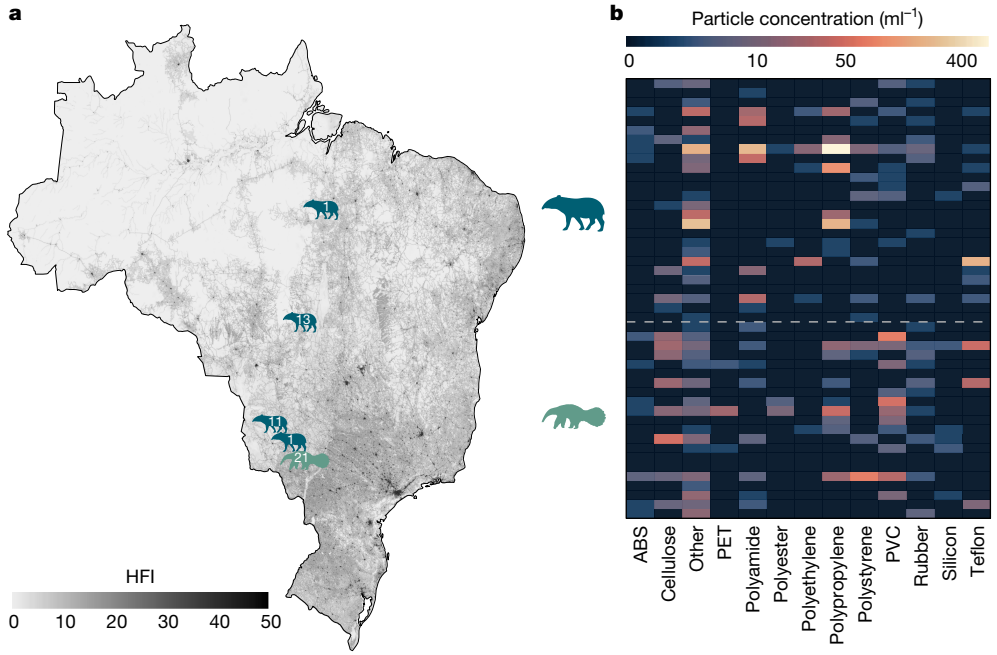


Fig. 1 | Overview of the dataset with microplastic characterization across species. a, Locations of the monitored lowland tapirs (blue, $n = 26$ animals) and giant anteaters (green, $n = 21$ animals) throughout Brazil, overlaid on top of the HFI. The numbers depict the sample sizes within each study area. **b**, Heat map depicting the concentration of the analysed microplastic polymers for lowland tapirs (blue) and giant anteaters (green). Each row in the heat map corresponds to an individual animal. Polymers categorized as 'other' were those that occurred at low abundance, and included polyvinyl butyralolyethyleneimine, poly(butylene terephthalate), polyvinylformal, polyacetal, polymethylpentene, polyurethane and polyethylene glycol. Giant anteater image credit: Steven Traver via PhyloPic (CC0 1.0); tapir image credit: Christophe Mallet via PhyloPic (CC0 1.0).

towards understanding the ecological and landscape-level factors that shape microplastic burdens in terrestrial species[29].

Here we integrate movement ecology, land-use data and in vivo contaminant measurements within the same individuals to investigate how the intensity and proximity of anthropogenic land-use change shape systemic microplastic burdens in terrestrial mammals. The role of anthropogenic disturbance in shaping internal plastic burdens is particularly pressing in regions facing escalating environmental pressures, such as Brazil, where the extent of anthropogenic land-use change since the turn of the century has substantially outpaced the global average[30,31] and deforestation, resource extraction, urbanization, agricultural intensification and an expanding road network are rapidly transforming the country's landscapes[30,32]. By pairing in vivo microplastic measurements with high-resolution Global Positioning System (GPS) tracking data, we provide quantitative evidence that links individual-level habitat use and human landscape modification to systemic microplastic burdens in free-ranging terrestrial wildlife.

Land use shapes microplastic burdens

Between February 2021 and November 2022, we collected blood samples and high-resolution GPS-based movement data from lowland tapirs (*Tapirus terrestris*; $n = 26$) and giant anteaters (*Myrmecophaga tridactyla*; $n = 21$) sampled at the Arc of Deforestation in the Amazon, an agricultural mosaic in the Cerrado, and a relatively undisturbed cattle ranch in the Pantanal (Fig. 1a and Extended Data Table 1). For each individual, we quantified blood microplastic concentrations and polymer profiles using confocal Raman spectroscopy, detecting particles larger than 1 µm. We then paired these data on in vivo microplastic burdens with the GPS tracking data to understand how inter-individual differences in habitat use and disturbance exposure shaped internal microplastic burdens. In particular, we quantified each individual's exposure to human disturbance through the Human Footprint Index (HFI), a globally standardized measure of cumulative anthropogenic pressure ranging from 0 (undisturbed) to 50 (most heavily modified)[33]. We also examined local-scale effects through each animal's proximity to the nearest human development (that is, the built environment including urban areas, mining infrastructure and power plants)[34] and waste management facilities[34].

Across all samples, we identified a total of 17,165 particles with a hit quality index (HQI) > 75, of which 2,815 (16.4%) were identified as microplastic. Microplastics were near-ubiquitous and found in the blood of all but four animals (three giant anteaters and one tapir), but systemic concentrations varied markedly across individuals (mean: 73.8 particles per ml; range 0 to 1,211.3 particles per ml). Lowland tapirs had the highest microplastic burdens (98.9 particles per ml; 95% confidence interval 52.0–188.0 particles per ml), followed by giant anteaters (42.8 particles per ml; 95% confidence interval 26.7–68.6 particles per ml); however, concentrations did not differ significantly between species ($\beta = 0.84$, $t = 1.88$, $P = 0.067$). Tapirs and giant anteaters did differ in polymer composition (Fig. 1b, Extended Data Fig. 1 and Supplementary Information), with additional inter-individual variation detailed in the Supplementary Discussion and Extended Data Fig. 2. Although comparable data on systemic microplastic burdens are not presently available for other species of terrestrial wildlife, the mean concentration of 73.8 particles per ml found in these animals is within the range reported in human blood using spectroscopic methods[35] (1.9 to 108 particles per ml).

Across species and sampling sites, individual differences in blood microplastic burdens were consistently associated with anthropogenic disturbance. Of the 47 animals from which blood samples were collected, 40 had sufficient GPS tracking data for inclusion in the habitat use analyses. These animals spanned a wide gradient of human pressure (Fig. 2a), with the maximum HFI individuals experienced ranging from as low as 2.6 to 40.5. The home ranges of these animals were 12.6 km from the nearest human development on average, ranging from 95 m to 67.4 km. There was a significant positive relationship between blood microplastic concentrations and the maximum HFI within an animal's

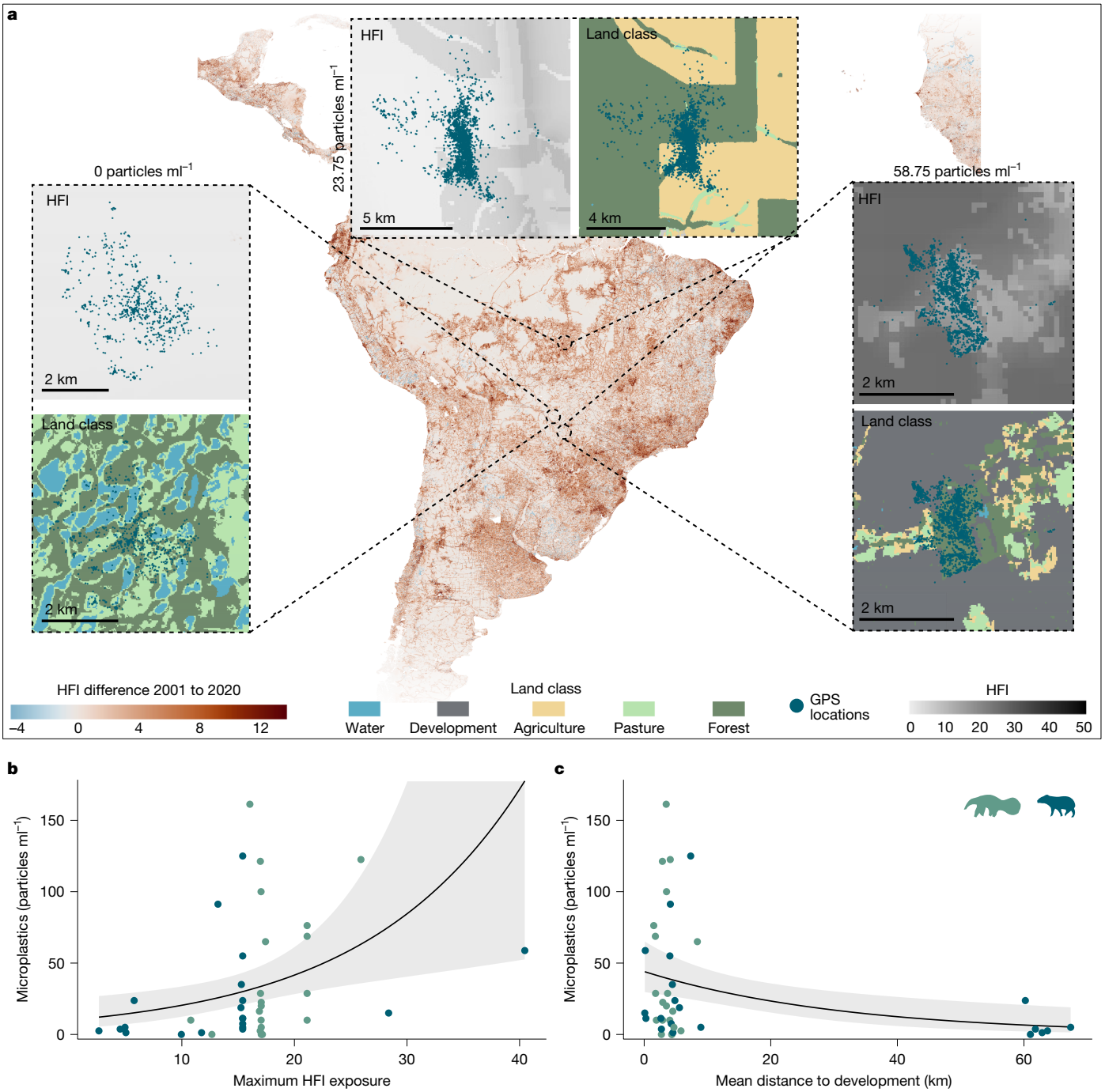


Fig. 2 | Relationships between habitat use and blood microplastic concentrations in the 40 animals for which we had GPS tracking data. **a**, Map of the difference in the HFI between 2001 and 2020; examples of HFI and animal movement, as well as land-use class and animal movement data (scatter points), are shown for animals with high, medium and low blood microplastic concentrations. **b**,**c**, The scatter plots ($n = 20$ lowland tapirs and 20 giant anteaters) show the relationships between microplastic concentrations and the maximum HFI in home range (**b**; $\beta = 0.07$, $t = 2.66$, $P = 0.011$) and the mean distance to development (**c**; $\beta = -0.032$, $t = -2.94$, $P = 0.0057$). Lines in **b**,**c** show the fitted population-level trend from a hierarchical generalized linear model (Tweedie distribution; log link) with species-specific random intercepts and slopes; shaded bands are 95% confidence intervals. *P* values are based on two-sided tests, with no correction for multiple comparisons; coefficients are on the link scale. Giant anteater image credit: Steven Traver via PhyloPic (CC0 1.0); tapir image credit: Christophe Mallet via PhyloPic (CC0 1.0).

home range ($\beta = 0.07$, $t = 2.66$, $P = 0.011$; Fig. 2b), although weighted mean HFI exposure was non-significant ($\beta = 0.061$, $t = 1.73$, $P = 0.092$; Extended Data Fig. 3).

Although these results highlight how direct exposure to human-modified landscapes shapes internal microplastic burdens, plastic pollution is a transboundary issue with complex dispersal pathways[36]. Atmospheric deposition and waterborne transport are likely contributors, as airborne microplastics from urban, industrial and agricultural sources can travel long distances before settling in remote ecosystems, and rainfall runoff, river discharge and seasonal flooding redistribute particles across landscapes to habitats far from their original sources[2–5,7,37]. Focusing on direct HFI exposure alone can obscure such effects. Indeed, we found that the local-scale effects of human land use were particularly important in shaping the systemic microplastic

concentrations of the monitored animals, with significant effects of distance to development ($\beta = -0.032$, $t = -2.94$, $P = 0.0057$) and distance to the nearest waste management facility ($\beta = -0.026$, $t = -2.73$, $P = 0.0096$) (Fig. 2c and Extended Data Fig. 3). Additional data on giant armadillos (*Priodontes maximus*) living in the Pantanal corroborate this trend (see Supplementary Discussion). These relationships were all robust to sensitivity analyses (Extended Data Tables 2 and 3 and Supplementary Discussion) and highlight the role of anthropogenic land use in driving species' exposure to plastic pollution. The polymer profiles also varied across sampling sites in patterns that were broadly consistent with the dominant human activities at each site (Extended Data Figs. 4 and 5 and Supplementary Discussion).

Microplastics scale with human pressure

Recent estimates[38] reveal that the mean global HFI increased from 5.26 in 2001 to 6.63 in 2020, representing a 26% increase. This trend in land-use change was even more pronounced in Brazil, where the HFI rose by 42% over the same period, from 4.17 to 5.92. Problematically, anthropogenic land-use expansion often outpaces the development of waste management infrastructure[39,40]. This infrastructural gap leaves regions experiencing the most rapid change the least equipped to contain plastic waste. Across large parts of rural and interior Brazil, for example, solid waste collection remains inadequate and wastewater treatment is limited or absent altogether[41–43]. The plastic materials tied to the expanding human footprint thus have few barriers preventing them from becoming highly mobile environmental pollutants[42]. The relationship between human disturbance and blood microplastic concentrations identified here suggests that microplastic burdens in terrestrial wildlife will continue to rise as land-use change intensifies. Notably, even at an HFI of zero the model predicted blood microplastic concentrations of 10.5 particles per ml (95% confidence interval 4.6–24.2 particles per ml; intercept: $\beta = 2.36$, $t = 5.58$, $P < 0.001$). While we can not discount the potential that this non-zero intercept was the result of an unmodelled non-linear relationship at low HFI exposure, it does provide support that direct exposure to human-modified landscapes is unlikely to be the sole driver of systemic microplastic burdens. The seemingly pervasive reach of microplastic pollution is most strikingly illustrated by our findings from the animals in the Pantanal. The Pantanal is the world's largest and most pristine wetland, supporting an extraordinary diversity of wildlife within a relatively undisturbed landscape[44]. Unlike other biomes in Brazil, much of the Pantanal has remained ecologically intact owing to its remote location, limited infrastructure and seasonal flooding, which naturally regulate many human activities. Yet, we found microplastics in the blood of all of the individuals we sampled in the Pantanal, despite these animals living more than 65 km from the nearest development and more than 112 km from the nearest waste management facility. This finding is corroborated by several recent studies that reported substantial concentrations of microplastics in both aquatic environments and sediments throughout the Pantanal[45–47], with the highest levels of microplastics (up to 1,174.2 items per m^2) found near rivers flowing from urban areas[46]. The presence of microplastics in the blood of animals living many tens of kilometres from the nearest development or waste facility highlights how microplastics are a threat not only to wildlife with direct exposure to human-modified landscapes, but also to species across even the most remote and ecologically intact environments[8]. Developing a mechanistic understanding of the pathways through which microplastics reach remote terrestrial ecosystems will be essential for protecting wildlife from this highly mobile pollutant. Although environmental sampling across these sites would strengthen the causal inference of these relationships by directly linking environmental polymer profiles to those detected in blood, isolation protocols for chemically diverse samples such as blood and soil complicate spectroscopy-based comparisons[48,49]. Paired blood–environment sampling designs thus represent a productive, albeit challenging path forward.

By combining in vivo microplastic measurements with fine-scale movement data and high-resolution landscape disturbance indices, our study moves terrestrial microplastic research beyond detection surveys towards a spatially informed quantitative framework for predicting wildlife burdens from landscape context. This approach revealed how individual habitat use and anthropogenic land-use change interact to shape wildlife exposure to microplastics, and is readily transferable to other species and regions, offering a scalable tool for identifying vulnerable populations and informing targeted conservation responses. While no ecosystem is likely to be entirely free of microplastics[50], we did find that animals in less disturbed habitats carried substantially lower burdens than those in close proximity to human infrastructure. These findings suggest that management efforts aimed at limiting animals' exposure to human-modified environments and reducing their proximity to development and waste management infrastructure can serve to reduce the microplastic burdens carried by wildlife.

Online content

Any methods, additional references, Nature Portfolio reporting summaries, source data, extended data, supplementary information, acknowledgements, peer review information; details of author contributions and competing interests; and statements of data and code availability are available at https://doi.org/10.1038/s41586-026-11285-x.

1. de Souza Machado, A. A., Kloas, W., Zarfl, C., Hempel, S. & Rillig, M. C. Microplastics as an emerging threat to terrestrial ecosystems. *Global Change Biol.* **24**, 1405–1416 (2018).
2. Wright, S. L., Ulke, J., Font, A., Chan, K. L. A. & Kelly, F. J. Atmospheric microplastic deposition in an urban environment and an evaluation of transport. *Environ. Int.* **136**, 105411 (2020).
3. Allen, S. et al. Atmospheric transport and deposition of microplastics in a remote mountain catchment. *Nat. Geosci.* **12**, 339–344 (2019).
4. Hu, L., Fu, J., Wang, S., Xiang, Y. & Pan, X. Microplastics generated under simulated fire scenarios: Characteristics, antimony leaching, and toxicity. *Environ. Pollut.* **269**, 115905 (2021).
5. Moodley, T., Abunama, T., Kumari, S., Amoah, D. & Seyam, M. Applications of mathematical modelling for assessing microplastic transport and fate in water environments: a comparative review. *Environ. Monit. Assess.* **196**, 667 (2024).
6. Patterson, J. et al. Impact of flooding events on microplastic distribution from rivers to coastal areas: a case study from Tuticorin, Southeast India. *Mar. Pollut. Bull.* **221**, 118471 (2025).
7. Lahon, J. & Handique, S. Impact of flooding on microplastic abundance and distribution in freshwater environment: a review. *Environ. Sci. Pollut. Res.* **30**, 118175–118191 (2023).
8. Bergmann, M. et al. White and wonderful? Microplastics prevail in snow from the Alps to the Arctic. *Sci. Adv.* **5**, eaax1157 (2019).
9. Redko, V., Wolska, L. & Cieślak-Piotrowicz, A. Alteration and progressive degradation of plastic waste in a polish operational landfill analysed over 60 years. *Commun. Earth Environ.* **5**, 565 (2024).
10. Chamas, A. et al. Degradation rates of plastics in the environment. *ACS Sustain. Chem. Eng.* **8**, 3494–3511 (2020).
11. Horton, A. A., Walton, A., Spurgeon, D. J., Lahive, E. & Svendsen, C. Microplastics in freshwater and terrestrial environments: Evaluating the current understanding to identify the knowledge gaps and future research priorities. *Sci. Total Environ.* **586**, 127–141 (2017).
12. Fleury, J.-B. & Baulin, V. A. Microplastics destabilize lipid membranes by mechanical stretching. *Proc. Natl Acad. Sci. USA* **118**, e2104610118 (2021).
13. Liu, L. et al. Cellular internalization and release of polystyrene microplastics and nanoplastics. *Sci. Total Environ.* **779**, 146523 (2021).
14. Deng, Y., Zhang, Y., Lemos, B. & Ren, H. Tissue accumulation of microplastics in mice and biomarker responses suggest widespread health risks of exposure. *Sci. Rep.* **7**, 46687 (2017).
15. Li, L., Zhou, Q., Yin, N., Tu, C. & Luo, Y. Uptake and accumulation of microplastics in an edible plant. *Chin. Sci. Bull.* **64**, 928–934 (2019).
16. Lu, Y. et al. Uptake and accumulation of polystyrene microplastics in zebrafish (*Danio rerio*) and toxic effects in liver. *Environ. Sci. Technol.* **50**, 4054–4060 (2016).
17. Anbumani, S. & Kakkar, P. Ecotoxicological effects of microplastics on biota: a review. *Environ. Sci. Pollut. Res. Int.* **25**, 14373–14396 (2018).
18. Bahrani, F. et al. Occurrence of microplastics in edible tissues of livestock (cow and sheep). *Environ. Sci. Pollut. Res.* **31**, 22145–22157 (2024).
19. Thompson, R. C. et al. Twenty years of microplastic pollution research—what have we learned? *Science* **386**, eadl2746 (2024).
20. Huang, Z. et al. Microplastics in the Amur tiger's habitat: occurrence, characteristics, and risk assessment. *J. Hazard. Mater.* **493**, 138380 (2025).
21. Wu, T. et al. Microplastic pollution of threatened terrestrial wildlife in nature reserves of Qinling Mts., China. *Glob. Ecol. Conserv.* **51**, e02865 (2024).
22. Teampanpong, J. & Duengkae, P. Terrestrial wildlife as indicators of microplastic pollution in western Thailand. *PeerJ* **12**, e17384 (2024).

23. Clark, B. L. et al. Global assessment of marine plastic exposure risk for oceanic birds. *Nat. Commun.* **14**, 3665 (2023).
24. Zhang, Y. et al. Effects of land use and landscape on the occurrence and distribution of microplastics in soil, China. *Sci. Total Environ.* **847**, 157598 (2022).
25. Lwanga, E. H. et al. Review of microplastic sources, transport pathways and correlations with other soil stressors: a journey from agricultural sites into the environment. *Chem. Biol. Technol. Agric.* **9**, 20 (2022).
26. Raza, M., Lee, J.-Y. & Cha, J. Microplastics in soil and freshwater: understanding sources, distribution, potential impacts, and regulations for management. *Sci. Prog.* https://doi.org/10.1177/00368504221126676 (2022).
27. Plumptre, A. J. et al. Where might we find ecologically intact communities? *Front. For. Glob. Change* **4**, 626635 (2021).
28. MacLeod, M., Arp, H. P. H., Tekman, M. B. & Jahnke, A. The global threat from plastic pollution. *Science* **373**, 61–65 (2021).
29. Brand, J. A. et al. Advancing the spatiotemporal dimension of wildlife–pollution interactions. *Environ. Sci. Technol. Lett.* **12**, 358–370 (2025).
30. Albert, J. S. et al. Human impacts outpace natural processes in the Amazon. *Science* **379**, eabo5003 (2023).
31. Cabernard, L., Pfister, S. & Hellweg, S. Biodiversity impacts of recent land-use change driven by increases in agri-food imports. *Nat. Sustain.* **7**, 1512–1524 (2024).
32. Camara, G. et al. Impact of land tenure on deforestation control and forest restoration in Brazilian Amazonia. *Environ. Res. Lett.* **18**, 065005 (2023).
33. Sanderson, E. W. et al. The human footprint and the last of the wild. *BioScience* **52**, 891 (2002).
34. Souza, C. M. et al. Reconstructing three decades of land use and land cover changes in Brazilian biomes with Landsat Archive and Earth Engine. *Remote Sens.* **12**, 2735 (2020).
35. Lamoree, M. H. et al. Health impacts of microplastic and nanoplastic exposure. *Nat. Med.* **31**, 2873–2887 (2025).
36. Bank, M. S. & Hansson, S. V. The microplastic cycle: an introduction to a complex issue. in *Microplastic in the Environment: Pattern and Process* (ed. Bank, M. S.) 1–16 (Springer, 2022).
37. Evangeliou, N. et al. Atmospheric transport is a major pathway of microplastics to remote regions. *Nat. Commun.* **11**, 3381 (2020).
38. Gassert, F. et al. An operational approach to near real time global high resolution mapping of the terrestrial Human Footprint. *Front. Remote Sens.* **4**, 1130896 (2023).
39. Villarrubia-Gómez, P., Carney Almroth, B., Eriksen, M., Ryberg, M. & Cornell, S. E. Plastics pollution exacerbates the impacts of all planetary boundaries. *One Earth* **7**, 2119–2138 (2024).
40. Kibria, M. G., Masuk, N. I., Safayet, R., Nguyen, H. Q. & Mourshed, M. Plastic waste: challenges and opportunities to mitigate pollution and effective management. *Int. J. Environ. Res.* **17**, 20 (2023).
41. Lima, P. D. M., Morais, M. F. D., Constantino, M. A., Paulo, P. L. & Magralhães Filho, F. J. C. Environmental assessment of waste handling in rural Brazil: improvements towards circular economy. *Clean. Environ. Syst.* **2**, 100013 (2021).
42. Oliveira, B. O. S. D., Medeiros, G. A. D., Paes, M. X. & Mancini, S. D. Integrated municipal and solid waste management in the Amazon: addressing barriers and challenges in using the Delphi method. *Int. J. Environ. Impacts* **4**, 49–61 (2021).
43. Lino, F. A. M., Ismail, K. A. R. & Castañeda-Ayarza, J. A. Municipal solid waste treatment in Brazil: a comprehensive review. *Energy Nexus* **11**, 100232 (2023).
44. Schulz, C. et al. Physical, ecological and human dimensions of environmental change in Brazil's Pantanal wetland: synthesis and research agenda. *Sci. Total Environ.* **687**, 1011–1027 (2019).
45. Camargo, A. L. G. et al. Microplastics in sediments of the Pantanal Wetlands, Brazil. *Front. Environ. Sci.* **10**, 1017480 (2022).
46. De Faria, É. et al. Microsynthetics in waters of the South American Pantanal. *Front. Environ. Sci.* **10**, 878152 (2022).
47. De Faria, É. et al. Microplastics pollution in the South American Pantanal. *Case Stud. Chem. Environ. Eng.* **3**, 100088 (2021).
48. Hossain, R. & Sahajwalla, V. A comprehensive toolkit for micro- to nanoplastic analysis. *Environ. Sci. Nano* **13**, 122–149 (2026).
49. Gqomfa, B., Dlangamandla, C., Ntwampe, S. K., Chidi, B. S. & Maphanga, T. Current techniques for identifying, quantifying, and characterizing micro and nanoplastics with emphasis on strengths, limitations, and challenges. *Discov. Environ.* **3**, 282 (2025).
50. Lim, X. Microplastics are everywhere — but are they harmful? *Nature* **593**, 22–25 (2021).

Publisher's note Springer Nature remains neutral with regard to jurisdictional claims in published maps and institutional affiliations.

Open Access This article is licensed under a Creative Commons Attribution 4.0 International License, which permits use, sharing, adaptation, distribution and reproduction in any medium or format, as long as you give appropriate credit to the original author(s) and the source, provide a link to the Creative Commons licence, and indicate if changes were made. The images or other third party material in this article are included in the article's Creative Commons licence, unless indicated otherwise in a credit line to the material. If material is not included in the article's Creative Commons licence and your intended use is not permitted by statutory regulation or exceeds the permitted use, you will need to obtain permission directly from the copyright holder. To view a copy of this licence, visit http://creativecommons.org/licenses/by/4.0/.

© The Author(s) 2026

Methods

Sampling areas

Lowland tapirs. Lowland tapir (*T. terrestris*) samples were collected across three sites in Brazil. The agricultural mosaic site in the Cerrado was located between the municipalities of Nova Alvorada do Sul and Nova Andradina, in Mato Grosso do Sul State, Brazil (−21.99° N, −53.83° E). It features a mosaic of natural habitats, including Cerradão fragments, gallery forests and marshlands, which constitute approximately 12% of the study area. The remainder is heavily influenced by human activities, including agriculture (for example, sugarcane, soybean and corn), cattle ranching, eucalyptus plantations, highways and rural settlements. Precipitation exhibits marked seasonality, with approximately 70% of the total annual rainfall occurring between November and March[51].

The field site in the Pantanal was situated on Baía das Pedras Ranch, in the Nhecolândia Sub-Region of the Southern Pantanal, Municipality of Aquidauana, Mato Grosso do Sul State, Brazil (−19.33° N, −55.72° E). This private property spans 145 km^2 and comprises a mosaic of seasonally inundated grasslands, lakes, gallery forests, scrub, and deciduous forests. The Pantanal is a nearly pristine biome with a low human footprint, and is far removed from areas experiencing deforestation and other anthropogenic pressures. The ranch supports abundant wildlife and extensive cattle grazing on native grasses. The average annual temperature is 25 °C, and the annual rainfall is 1,185 mm.

The site in the Amazon was located at Tanguro Farm, a privately owned 103,000 ha property in Querência, Mato Grosso state, that sits at the transition between the Cerrado savanna and the Amazon rainforest along the southern Arc of Deforestation. Owned by AMAGGI, a major actor in Brazil's soybean industry, the farm comprises 59,000 ha (57%) of croplands (soybean, corn, and cotton) and 44,000 ha (43%) of legally protected forest reserves. This region is the driest portion of the Amazon basin and experiences a prolonged dry season (May–September) with annual rainfall of 1,700–2,200 mm. Forests in this region are shorter (~20 m) than the moist Amazon rainforest (~30 m). About 40% of the farm was cleared for pasture (1976–1992) and later converted to soy cultivation (2003–2010), leaving riparian forests surrounded by croplands.

Giant anteaters. The giant anteater (*M. tridactyla*) data collection was conducted in the Cerrado savanna of Mato Grosso do Sul state, Brazil, as part of the Anteaters and Highways Project (ICAS, www.icasconservation.org.br), which investigates wildlife-vehicle collisions and their impacts on wildlife populations. Sampling areas were located near two federal roads: BR-267 (−21.64° N, −53.51° E) and BR-262 (−20.86° N, −52.04° E). As described above, the study region is a mosaic landscape dominated by open areas, including grasslands, pastures, and croplands, interspersed with small remnants of native savanna and forest vegetation, as well as eucalyptus plantations[52].

Giant armadillos. In addition to the tapir and giant anteater data, we also obtained a smaller amount of data from three giant armadillos (*P. maximus*). The giant armadillo data collection was also conducted at the Baía das Pedras Lodge and Ranch in the Pantanal, which served as the base of operations for the Giant Armadillo Conservation Program (GACP).

Animal captures and GPS data acquisition

Ethics statement. All animal capture, handling, and blood sampling procedures were approved by the Brazilian Ministry of the Environment (MMA) and the Chico Mendes Institute for Biodiversity Conservation (ICMBio) under license numbers 14603-25 (lowland tapirs), 53798-18 (giant anteaters) and 27587-1 (giant armadillos). All procedures were performed in accordance with the terms of these licenses and with relevant national and institutional animal welfare guidelines. Chemical immobilization was performed under veterinary oversight, and all animals were released at their capture sites following full recovery.

Lowland tapirs. Lowland tapirs were captured using a combination of methods, including darting, following physical restraint in box-traps or pitfall traps, or darting from a distance. Box traps and pitfall traps were deployed in areas frequently visited by tapirs. Tapirs captured by these methods were anaesthetized intramuscularly with a combination of butorphanol (0.17 mg kg^{-1}), medetomidine (0.012 mg kg^{-1}) and ketamine (0.7 mg kg^{-1}). Reversal agents, including atipamezole (0.04 mg kg^{-1}) and naltrexone (0.35 mg kg^{-1}), were administered at the conclusion of procedures. For tapirs darted from a distance, anaesthetics included tiletamine-zolazepam (1.25 mg kg^{-1}), medetomidine (0.006 mg kg^{-1}), ketamine (0.6 mg kg^{-1}) and atropine (0.03 mg kg^{-1}). Darts (3 ml or 5 ml) were used to deliver anaesthetics. Midazolam (0.03 mg kg^{-1}) was administered 30 min later to maintain anaesthesia. Captured tapirs underwent a range of procedures, including subcutaneous microchip insertion, morphometric measurements, sex and age determination, physical examinations, blood sample collection and telemetry collar placement for adults.

Tapirs were equipped with GPS collars (Telonics TGW SOB and GPS IRIDIUM models) programmed to obtain hourly location fixes, with a median operational life of 15.4 months. Additional location data were collected from stationary tags placed in the Pantanal (n = 883) and Cerrado (n = 174) to calibrate the measurement error in the GPS datasets.

Giant anteaters. Giant anteaters were captured between February 2021 and November 2022 using motorized active searches between 15:00 and 17:00, when they exhibit higher diurnal activity due to colder temperatures[53,54]. Searches were conducted along dirt roads in open areas, with two team members stationed in the back of a truck to improve detectability. Upon spotting an individual, technicians approached the animal on foot and captures were performed using two long-handled dip nets (1.5 m handles, 0.7 m diameter hoops). Physical capture typically lasted around 1 min.

Captured giant anteaters were chemically immobilized, equipped with GPS radiotelemetry harnesses (Telonics) as previously described[55] and blood samples were collected. In brief, animals were anaesthetized using a protocol of butorphanol tartrate (Zoetis Indústria de Produtos Veterinários; 0.1 mg kg^{-1}), detomidine hydrochloride (Agener-União; 0.1 mg kg^{-1}) and midazolam hydrochloride (Cristália; 0.2 mg kg^{-1}), adapted from ref. 55. The induction period averaged 8.27 ± 4.78 min.

Giant armadillos. Giant armadillos were captured between February 2021 and November 2022, using a method tailored to their natural behaviour[56]. Researchers tracked footprints and signs of recent predation, such as termite mounds, to locate burrows. When a burrow was identified and confirmed to contain an armadillo (indicated by the entrance being sealed with sand), an iron funnel trap (jequi-type) was placed at the entrance. Once captured, animals were transported in iron-reinforced wooden crates and held overnight for nocturnal species, with procedures beginning the following morning at the capture site.

Captured giant armadillos were anaesthetized for the collection of blood samples and surgical implantation of intra-abdominal transmitters. Anaesthetic protocols included an intramuscular injection of butorphanol tartrate (0.1 mg kg^{-1}), detomidine hydrochloride (0.1 mg kg^{-1}), and midazolam hydrochloride (0.1 mg kg^{-1}) into the hind limbs. Before surgery, intradermal local anaesthesia with lidocaine hydrochloride (2 mg kg^{-1}, Eurofarma) was infiltrated into the infra-umbilical region. Ketamine hydrochloride (10 mg kg^{-1}) was administered intramuscularly as a supplementary anaesthetic immediately after the animals were completely washed. Transmitters (IMP 310 model, Telonics; 9.4 × 2.3 cm, 42 g, 36-month operational life) were surgically implanted within the abdominal cavity under sterile

conditions. Following surgery, anaesthesia was reversed using a combination of naloxone hydrochloride (0.02 mg kg^{-1}), yohimbine hydrochloride (0.125 mg kg^{-1}), and flumazenil (0.01 mg kg^{-1}). Armadillos were released at their capture sites upon recovery, typically remaining in their burrows for 24 to 120 h (average of 48 h) before emerging. Daily monitoring was conducted for 12–22 days post-release using telemetry receivers (model TR-4, Telonics) and VHF antennas (model RA-23K). After the initial monitoring period, armadillos were monitored monthly until the end of the transmitter's operational life.

Blood sample collection

Lowland tapirs. Approximately 10 ml of blood was collected within 20 min of immobilization via venipuncture of the medial saphenous or cephalic veins using a sterile glass vacutainer system (BD Vacutainer). Tapir captures were conducted in remote forest sites without access to field refrigeration. Blood samples were therefore stored in pre-cleaned glass collection tubes with no preservatives, sealed with clean aluminium foil and a metal cap to prevent contamination during storage, kept shaded at ambient temperature, and transferred to a −20 °C freezer on return to the base camp within 5–6 h.

Giant anteaters and giant armadillos. Blood samples (~5 ml) were collected approximately 20 min after induction from the cephalic or saphenous veins using a sterile vacutainer system with 23G or 25G needles (BD Vacutainer). Samples were transferred to pre-cleaned glass collection tubes with no preservatives, sealed with clean aluminium foil and a metal cap to prevent contamination during storage, kept refrigerated at 4 °C on site, and frozen at −20 °C within 12–24 h for subsequent processing. We note that blood samples were obtained from three individual giant armadillos, however we obtained repeat samples at two time points for two of these animals. Although these blood samples were processed individually, they were pooled (that is, averaged) in our statistical analyses.

Cold storage under the above-mentioned conditions is standard practice in microplastic analyses and does not affect particle abundance or polymer identity. Microplastics are chemically stable over these timescales, and method reviews emphasize that environmental samples containing microplastics are routinely stored at 4 °C for days to weeks prior to processing, or frozen at −20 °C for longer periods, without alteration of polymer composition (reviewed in ref. 57).

Microplastic isolation from blood

Blood microplastic isolation was performed following a protocol previously developed by our team[58–60]. Depending on the sampling date, blood samples were stored at −20 °C for ~1–22 months between collection (Feb 2021–Nov 2022) and digestion (Dec 2022). On the first day of isolation, 1 ml of each blood sample was placed in an Erlenmeyer flask along with 50 ml of 10% KOH solution (sample ratio of 1:50). The mixture was incubated on a shaker at 60 °C and 250 rpm for 24 h. After the initial 24-h incubation, 10 ml of 47% NaClO were added to each sample to achieve a final concentration of 7.7%. The samples were then incubated under the same conditions (60 °C and 250 rpm) for an additional 24 h.

Following the second day of digestion, all samples were filtered through a 47 mm polytetrafluoroethylene (PTFE) membrane with a 0.45 µm pore size (Merck Omnipore) and rinsed 3 times with filtered ultrapure water. The membranes containing the particles were then submerged in 50 ml of 20% HNO_3 and placed in an ultrasonic bath with sweep function at 100% power and 45 kHz frequency for 15 min to transfer the particles from the membrane to the solution. The samples were further incubated for 30 min at 40 °C and 250 rpm.

After removing the membranes, the samples underwent a 24-h incubation at 40 °C and 250 rpm. On the final day, the samples were filtered through a 13 mm PTFE membrane with a 0.45 µm pore size, rinsed three times with filtered ultrapure water, and mounted on glass slides for microscopy and spectroscopy analysis. The resulting filter membranes were then stored in pre-cleaned glass Petri dishes and analysed by Raman spectroscopy over the subsequent ~12 months (Jan–Dec 2023). After digestion, a proportion of non-plastic particulates remained on the membrane, such that microplastics accounted for an average of 16.4% of imaged particles with HQI > 75 (range 0–89.9%).

Quality assurance and quality control methods used throughout the process are detailed in the Supplementary Methods (see also Extended Data Figs. 6 and 7).

Confocal Raman analysis of particles

Microplastic identification and characterization were conducted using a confocal Raman microscope (alpha300 R, WITec) equipped with a UHTS 300 spectrometer (WITec) and a 532-nm laser. The microscope was operated using Control Five software, and the acquired data were processed with Project Five software to compensate for background noise and cosmic radiation signals.

As an initial step, a whole membrane image was captured using a 10× NA 0.25 Zeiss objective with the Area Stitching option. From this image, a specific field was selected for detailed imaging with a 50× NA 0.75 Zeiss objective, employing both the Area Stitching option and Z-stack autofocus. Particle identification was facilitated by the Particle Scout software, which enabled the acquisition of Raman spectra for all identified particles across the entire membrane. Raman spectra were then obtained using a 100× DIC NA 0.9 Zeiss objective, with a laser power of 10 mW, an accumulation of 4, and an integration time of 0.45 s. Spectra autofocus was used throughout the measurements. The acquired spectra were then compared against the S.T. Japan database (S.T. Japan Europe GmbH) and the SLoPP MPs Raman library[61] using the True Match-Integrated Raman Spectra Database Management software. Microplastic characterization was based on an automated, 3-step process that was optimized for spectra acquisition rather than image sharpness. This precluded the manual assessment of particle shape (for example, fibres or fragments) or colour. Only matches with an HQI greater than 75% were considered for further analysis.

HFI differences between 2001 and 2020

To assess changes in the HFI over time, we obtained and processed global HFI rasters at a 300 m resolution for the years 2001 and 2020 from the Wildlife Conservation Society Human Footprint dataset (https://wcshumanfootprint.org/). After ensuring projections and resolutions were consistent between the HFI rasters, a difference raster was generated by subtracting the 2001 HFI from the 2020 HFI to visualize areas of increasing and decreasing human influence. We cropped and masked the HFI rasters to remove areas outside of Brazil and then computed the mean HFI for 2001 and 2020, as well as the absolute differences. These analyses were conducted in R using the terra (v1.8-54)[62], sf (v1.0-21)[63,64], tmap (v4.0.0.9000)[65], fields (v16.3)[66], rnaturalearth (v1.0.1)[67], and geobr (v1.9.1)[68] packages.

Animal movement analysis

Movement data pre-processing. Before analysis, we pre-processed the GPS location data in order to calibrate the measurement error and filter outliers. Pre-processing was done via the methods implemented in the R package ctmm (v1.2.1)[69]. For each location estimate, the GPS trackers recorded a unitless Horizontal Dilution of Precision (HDOP), a value which is a measure of the accuracy of each positional fix. We converted the HDOP values into calibrated errors by specifying 20-m error at an HDOP of 1 for 2D fixes, and 10-m error at an HDOP of 1 for the 3D fixes[70]. For each individual dataset, we then removed outliers based on error-informed distance from the median location, and the minimum speed required to explain each location's displacement. Through this process we identified a total of 16,656 outliers, which represented ca. 3.55% of the total 469,410 locations. After filtering outliers, the final dataset consisted of 343,913 GPS locations across 20 individual

giant anteaters, 6,072 GPS locations across 2 individual giant armadillos, and 102,769 GPS locations across 20 individual lowland tapirs.

Movement modelling. For each of the tracked animals, we used a continuous-time approach to estimate their movement rates and home ranges, enabling robust comparisons across individuals[71]. We first fitted a series of continuous-time stochastic process movement models to the location data. Parameters were estimated using perturbative-hybrid residual maximum likelihood (pHREML)[72], and identified the best model via small-sample-sized-corrected Akaike's information criterion (AICc). From both visual inspections of the semi-variograms, and the parameters of the fitted movement models, all animals occupied stable home ranges throughout the monitoring period with no indication of range shifts or large-scale dispersal events.

From the selected models, we estimated each animal's diffusion rate (in $km^2\ day^{-1}$) as a measure of their movement rate. We next estimated each animal's home range, using autocorrelated kernel density estimation (AKDE)[73]. AKDE home range estimates were conditioned on the autocorrelation structure of the fitted movement model, and we implemented the small-sample-size bias correction of Fleming & Calabrese (2017)[74], as well as the optimal weighting of Fleming et al. (2018)[75] to correct for uneven sampling. Home range areas (in km^2) were estimated as the area contained within the polygon delimited by the 95% isopleth of the probability density.

We estimated the mean and maximum HFI within each individual's home range. HFI is an aggregate measure of human disturbance that ranges from 0 in natural habitats to 50 in the most anthropogenically modified habitats[33]. A raster of HFI data with a spatial resolution of 100 m was obtained from Gassert et al.[38]. The weighted mean HFI within an individual's home range was estimated by calculating the weighted arithmetic mean of HFI values:

$$\mathrm{HFI} = \frac{\sum_{u=1}^{n} w_u \mathrm{HFI}_u}{\sum_{u=1}^{n} w_u}$$

with weights (w_u) determined by the probability density at each location u. Maximum HFI exposure was estimated by identifying the maximum value of HFI within each animal's home range. We also estimated more nuanced patterns of habitat use via the MapBiomas database[34], which details land use throughout Brazil at a spatial resolution of 10 m. We focused on habitats classified as water, development, agriculture, pasture, and native forest, which represented the majority of the land classes within the monitored animals' home ranges. The proportions of each of these land classes within each animal's home range were again estimated by calculating the weighted arithmetic mean. Lastly, we used the MapBiomas land classification data, the Rocky Mountain Institute (RMI), and the Waste Methane Assessment Platform 1.5.0, 2025 (https://wastemap.earth) to generate spatial rasters of distance to development, and distance to the nearest waste management facility (both in m). Development was a compound measure that captured the built environment, and was composed of the MapBiomas collection 10 classes: urban areas (24), mining (30), photovoltaic power plants (75), and other non-vegetated areas (25). From these spatial data, we estimated each animal's mean distance to development and to the nearest waste management facility, estimated by calculating the weighted arithmetic mean.

Statistical modelling

To study how human land-use change shaped blood microplastic concentrations, we fit hierarchical generalized linear regression models using the methods implemented in the mgcv package (v1.9-1)[76]. Because the microplastic concentrations scaled between [0,∞], we used a Tweedie distribution with a log link for the error distribution[77], with parameters estimated via restricted maximum likelihood (REML). The regression models testing for correlations between individual habitat use and microplastic concentrations included a population-level effect, as well as random intercepts and slopes for each of the species, with the following general form

$$\begin{aligned} \text{Blood microplastics}_i &\sim \text{Tweedie}(\mu_i, p) \\ \log(\mu_i) &= \beta_0 + \beta x_i + u_{s[i]} + v_{s[i]} x_i \\ u_s &\sim \mathcal{N}(0, \sigma_u^2),\ v_s \sim \mathcal{N}(0, \sigma_v^2), \end{aligned}$$

where β_0 represents the population-level intercept, β is the population-level slope, $u_{s[i]}$ is the species-specific random intercept, $v_{s[i]}$ is the species-specific random slope, and $s[i]$ indexes the species of individual i. This structure was used for all of the habitat covariates x_i. From these models, inference was then made on the population-level trend.

All analyses were conducted in R (v4.3.3). Weighted means and proportions of land-use exposure were computed with the weights package (v1.0.4). Figures were produced with ggplot2 (v3.5.2), ggspatial (v1.1.9), tidyterra (v0.7.0), rphylopic (v1.5.0; animal silhouettes), fmsb (v0.7.6) and gridExtra (v2.3).

Statistics and reproducibility

No statistical method was used to predetermine sample size. Sample sizes were determined by the number of animals that could be safely captured during the study period (February 2021 to November 2022) given the logistical constraints of live-capturing large, threatened, free-ranging mammals under national permits, and all animals captured during this period were sampled. This was an observational field study, so randomization was not applicable; animals were not allocated to experimental groups, and exposure to human land use was determined by each individual's own space use. The investigators were not blinded to species or sampling site during laboratory processing or analysis; however, particle detection and polymer identification were automated (Particle Scout and True Match software) and based on a fixed spectral-match threshold (HQI > 75%), which limits observer bias. Each animal contributed one blood sample, with the exception of two giant armadillos sampled at two time points, whose values were averaged before analysis. Seven animals lacked sufficient GPS tracking data and were excluded from the habitat use models but retained in descriptive analyses. Samples were processed in two batches, each with a procedural blank (Supplementary Methods); all lowland tapir samples were processed in the same batch. The polymer-integrity test shown in Extended Data Fig. 6 was repeated three times independently with similar results.

Reporting summary

Further information on research design is available in the Nature Portfolio Reporting Summary linked to this article.

Data availability

The blood microplastics data (particle-level measurements, polymer identifications and per-individual summaries underlying Figs. 1 and 2, Extended Data Figs. 1, 2 and 4–7 and Extended Data Tables 1–3), raw GPS tracking data, and the per-individual movement and land-use summaries (underlying Fig. 2 and Extended Data Fig. 3) are available at https://doi.org/10.6084/m9.figshare.34001445 (ref. 78) and on GitHub (https://github.com/QuantitativeEcologyLab/microplastics_brazil). This study also used the following publicly available datasets: the 100 m HFI[79] (https://source.coop/repositories/vizzuality/hfp-100/description); the Wildlife Conservation Society 300 m Human Footprint rasters for 2001 and 2020 (https://wcshumanfootprint.org/data-access); MapBiomas Brazil Collection 10 land use and land cover maps (https://brasil.mapbiomas.org/, downloads at https://brasil.mapbiomas.org/en/downloads/); waste management facility locations from the Waste Methane Assessment Platform (WasteMAP)

v1.5.0, developed by RMI and Clean Air Task Force (https://wastemap.earth); and Natural Earth (https://www.naturalearthdata.com) and geobr[68] basemap data. Raman spectra were matched against the SLoPP library[61] (openly available) and the S.T. Japan commercial spectral database (S.T. Japan Europe GmbH), which is available under licence from the vendor. Source data are provided with this paper.

Code availability

The code and data required to reproduce all of the analyses and figures in the manuscript are openly available at: https://github.com/QuantitativeEcologyLab/microplastics_brazil, and are permanently archived at https://doi.org/10.6084/m9.figshare.34001445 (ref. 78).

51. Andrade, R. G., Sediyama, G. C., Paz, A. R. D., Lima, E. D. P. & Facco, A. G. Geotecnologias aplicadas à avaliação de parâmetros biofísicos do Pantanal. *Pesq. Agropec. Bras.* **47**, 1227–1234 (2012).
52. Ascensão, F., Ribeiro, Y. G. G., Campos, Z., Yogui, D. R. & Desbiez, A. L. J. Forecasting seasonal peaks in roadkill patterns for improving road management. *J. Environ. Manage.* **321**, 115903 (2022).
53. Di Blanco, Y. E., Spørring, K. L. & Di Bitetti, M. S. Daily activity pattern of reintroduced giant anteaters (*Myrmecophaga tridactyla*): effects of seasonality and experience. *Mammalia* **81**, 11–21 (2017).
54. Giroux, A. et al. The role of environmental temperature on movement patterns of giant anteaters. *Integr. Zool.* **17**, 285–296 (2022).
55. Kluyber, D. et al. Physical capture and chemical immobilization procedures for a mammal with singular anatomy: the giant anteater (*Myrmecophaga tridactyla*). *Eur. J. Wildl. Res.* **67**, 67 (2021).
56. Kluyber, D., Pinho Gomez Lopez, R., Massocato, G., Attias, N. & Léonard Jean Desbiez, A. Anesthesia and surgery protocols for intra-abdominal transmitter placement in four species of wild armadillo. *J. Zoo Wildl. Med.* **51**, 514–526 (2020).
57. Nayebi, B., Khurana, P., Pulicharla, R., Karimpour, S. & Brar, S. K. Preservation, storage, and sample preparation methods for freshwater microplastics – a comprehensive review. *Environ. Sci. Adv.* **2**, 1060–1081 (2023).
58. Grechi, N., Ferronato, G. A., Devkota, S. & Ferraz, M. A. M. M. Microplastics are detected in bull epididymal sperm and polystyrene microparticles impair sperm fertilization. *Biol. Reprod.* **111**, 1341–1351 (2024).
59. Grechi, N. et al. Microplastics are present in women's and cows' follicular fluid and polystyrene microplastics compromise bovine oocyte function in vitro. *eLife* **12**, RP86791 (2023).
60. Noonan, M. J., Grechi, N., Mills, C. L., De, A. M. M. & Ferraz, M. Microplastics analytics: why we should not underestimate the importance of blank controls. *Micropl. Nanopl.* **3**, 17 (2023).
61. Munno, K., De Frond, H., O'Donnell, B. & Rochman, C. M. Increasing the accessibility for characterizing microplastics: introducing new application-based and spectral libraries of plastic particles (SLoPP and SLoPP-E). *Anal. Chem.* **92**, 2443–2451 (2020).
62. Hijmans, R. J., Brown, A., Barbosa, A. M., Cordano, E. & Dyba, K. terra: spatial data analysis. *GitHub* https://github.com/rspatial/terra (2024)
63. Pebesma, E. Simple features for R: standardized support for spatial vector data. *R J.* **10**, 439 (2018).
64. Pebesma, E. & Bivand, R. *Spatial Data Science: With Applications in R* (Chapman and Hall/CRC, 2023).
65. Tennekes, M. tmap: thematic maps in *R. J. Stat. Softw.* https://doi.org/10.18637/jss.v084.i06 (2018).
66. Nychka, D., Furrer, R., Paige, J. & Sain, S. fields: tools for spatial data. R package v.16.3 https://cran.r-project.org/package=fields (CRAN, 2021).
67. Massicotte, P. & South, A. rnaturalearth: world map data from Natural Earth. R package v.1.0.1 https://cran.r-project.org/package=rnaturalearth (CRAN, 2023).
68. Pereira, R. & Goncalves, C. geobr: download official spatial data sets of Brazil. R package v.1.9.1 https://cran.r-project.org/web/packages/geobr/index.html (CRAN, 2024).
69. Calabrese, J. M., Fleming, C. H. & Gurarie, E. ctmm: an R package for analyzing animal relocation data as a continuous-time stochastic process. *Methods Ecol. Evol.* **7**, 1124–1132 (2016).
70. Fleming, C. H. et al. A comprehensive framework for handling location error in animal tracking data. Preprint at *bioRxiv* https://doi.org/10.1101/2020.06.12.130195 (2020).
71. Noonan, M. J. et al. Scale-insensitive estimation of speed and distance traveled from animal tracking data. *Mov. Ecol.* **7**, 35 (2019).
72. Fleming, C. H., Noonan, M. J., Medici, E. P. & Calabrese, J. M. Overcoming the challenge of small effective sample sizes in home-range estimation. *Methods Ecol. Evol.* **10**, 1679–1689 (2019).
73. Fleming, C. H. et al. Rigorous home range estimation with movement data: a new autocorrelated kernel density estimator. *Ecology* **96**, 1182–1188 (2015).
74. Fleming, C. H. & Calabrese, J. M. A new kernel density estimator for accurate home-range and species-range area estimation. *Methods Ecol. Evol.* **8**, 571–579 (2017).
75. Fleming, C. H. et al. Correcting for missing and irregular data in home-range estimation. *Ecol. Appl.* **28**, 1003–1010 (2018).
76. Wood, S. N. mgcv: Mixed GAM computation vehicle with automatic smoothness estimation. R package v.1.9-1 https://doi.org/10.32614/CRAN.package.mgcv (CRAN, 2023).
77. Tweedie, M. C. K. An index which distinguishes between some important exponential families. In *Proc. Indian Statistical Institute Golden Jubilee International Conference* 579–604 (Indian Statistical Institute, 1984).
78. de Almeida Monteiro Melo Ferraz, M. et al. Data from: Human land use drives microplastic abundance in terrestrial wildlife. *Figshare* https://doi.org/10.6084/m9.figshare.34001445 (2026).
79. Mazzariello, J. & Gassert, F. Global 100 m Terrestrial Human Footprint (HFP-100). *Dryad* https://doi.org/10.5061/dryad.ttdz08m1f (2023).

Acknowledgements We acknowledge the many field and laboratory technicians who assisted with the data collection. We thank the members of The University of British Columbia, Okanagan's Biodiversity, Resilience and Ecosystem Services (BRAES) Institute, who provided invaluable feedback on earlier drafts of the manuscript. The study of tapir health is a long-term component of the Lowland Tapir Conservation Initiative (LTCI), Instituto de Pesquisas Ecológicas (IPÊ), Brazil, which has institutional support from the IUCN SSC Tapir Specialist Group, the Association of Zoos and Aquariums Tapir Taxon Advisory Group and the European Association of Zoos and Aquariums Tapir Taxon Advisory Group, and has been funded by over 50 zoological institutions, 20 NGOs and foundations, 11 corporations and private individuals. This study is also part of the long-term xenarthran ecological and health assessment initiatives of the Wild Animal Conservation Institute (ICAS), Brazil, and we thank all supporters of the Anteaters and Highways Project (https://www.icasconservation.org.br/projects/giant-anteater/?lang=en).

Author contributions M.d.A.M.M.F. and M.J.N. conceived the study. M.d.A.M.M.F., N.G. and M.P.M. performed all microplastics isolation and analysis, carried out in the laboratory of M.P.M. E.Y.L. analysed the movement and habitat use data together with M.J.N. and J.M.C. G.S., M.H.A., F.C.J., D.K., A.L.J.D. and E.P.M. carried out the field work, including animal capture, handling and blood and GPS-collar sample collection. M.d.A.M.M.F., N.G., E.Y.L., M.J.N., G.S., A.T.C., M.H.A., F.C.J., D.K., J.M.C. and M.P.M. contributed to the methodology. M.d.A.M.M.F. and M.J.N. produced the visualizations. M.d.A.M.M.F., A.L.J.D., E.P.M., G.M., M.P.M. and M.J.N. acquired funding and administered the project. M.d.A.M.M.F., A.L.J.D., G.M., J.M.C., M.P.M. and E.P.M. supervised the work. M.d.A.M.M.F. and M.J.N. wrote the original draft. All authors reviewed the article and provided feedback.

Funding M.J.N. discloses support for the research of this work from the Natural Sciences and Engineering Research Council of Canada (NSERC) (Discovery Grant RGPIN-2021-02758) and the Canada Foundation for Innovation (42111). M.d.A.M.M.F. discloses support for the research of this work from the LMU Excellence Fund, funded by the Federal Ministry of Education and Research (BMBF) and the Free State of Bavaria under the Excellence Strategy of the Federal Government and the Länder. J.M.C. discloses support for the research of this work from the Center for Advanced Systems Understanding (CASUS), which is financed by the German Federal Ministry of Education and Research (BMBF) and by the Saxon Ministry for Science, Culture and Tourism (SMWK) with tax funds on the basis of the budget approved by the Saxon State Parliament. E.P.M. discloses support for the research of this work from the Lowland Tapir Conservation Initiative (LTCI), Instituto de Pesquisas Ecológicas (IPÊ). A.L.J.D. discloses support for the research of this work from the Wild Animal Conservation Institute (ICAS) through the Anteaters and Highways Project. M.H.A., A.T.C., F.C.J., N.G., D.K., E.Y.L., M.P.M., G.S. and G.M. declare no relevant funding. Open access funding provided by Ludwig-Maximilians-Universität München.

Competing interests The authors declare no competing interests.

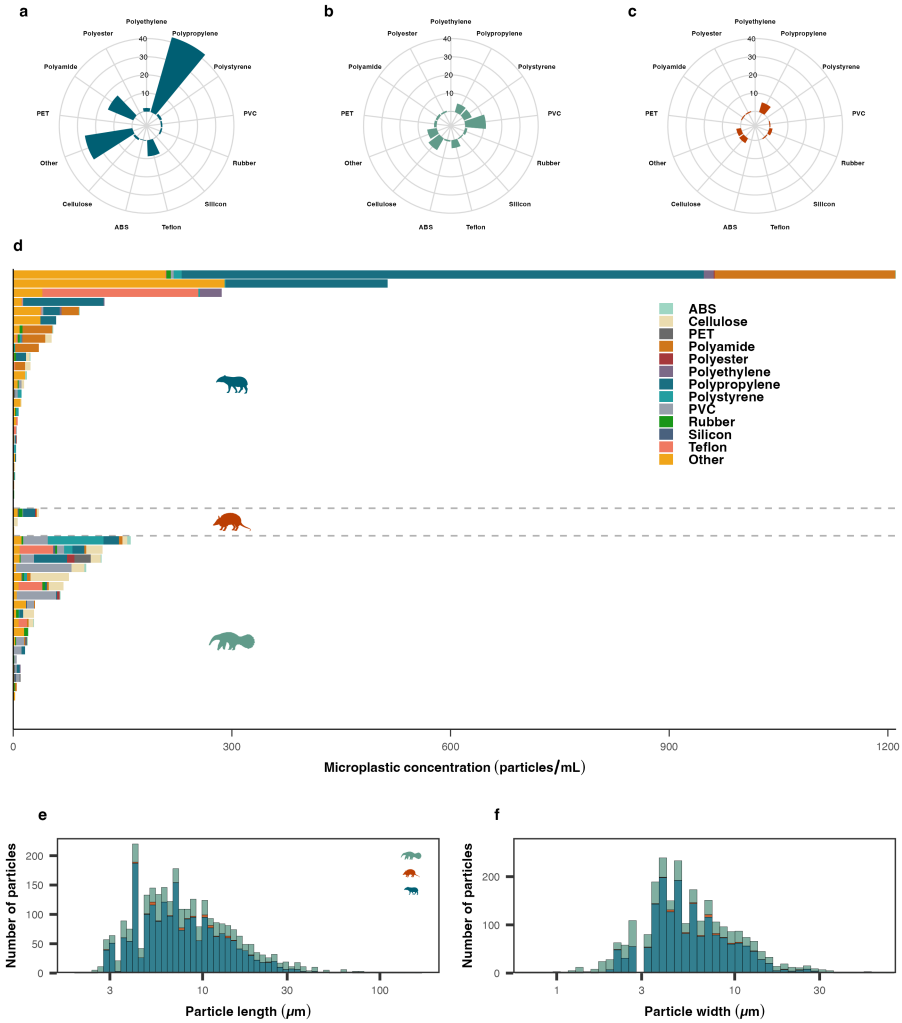
Additional information

Supplementary information The online version contains supplementary material available at https://doi.org/10.1038/s41586-026-11285-x.

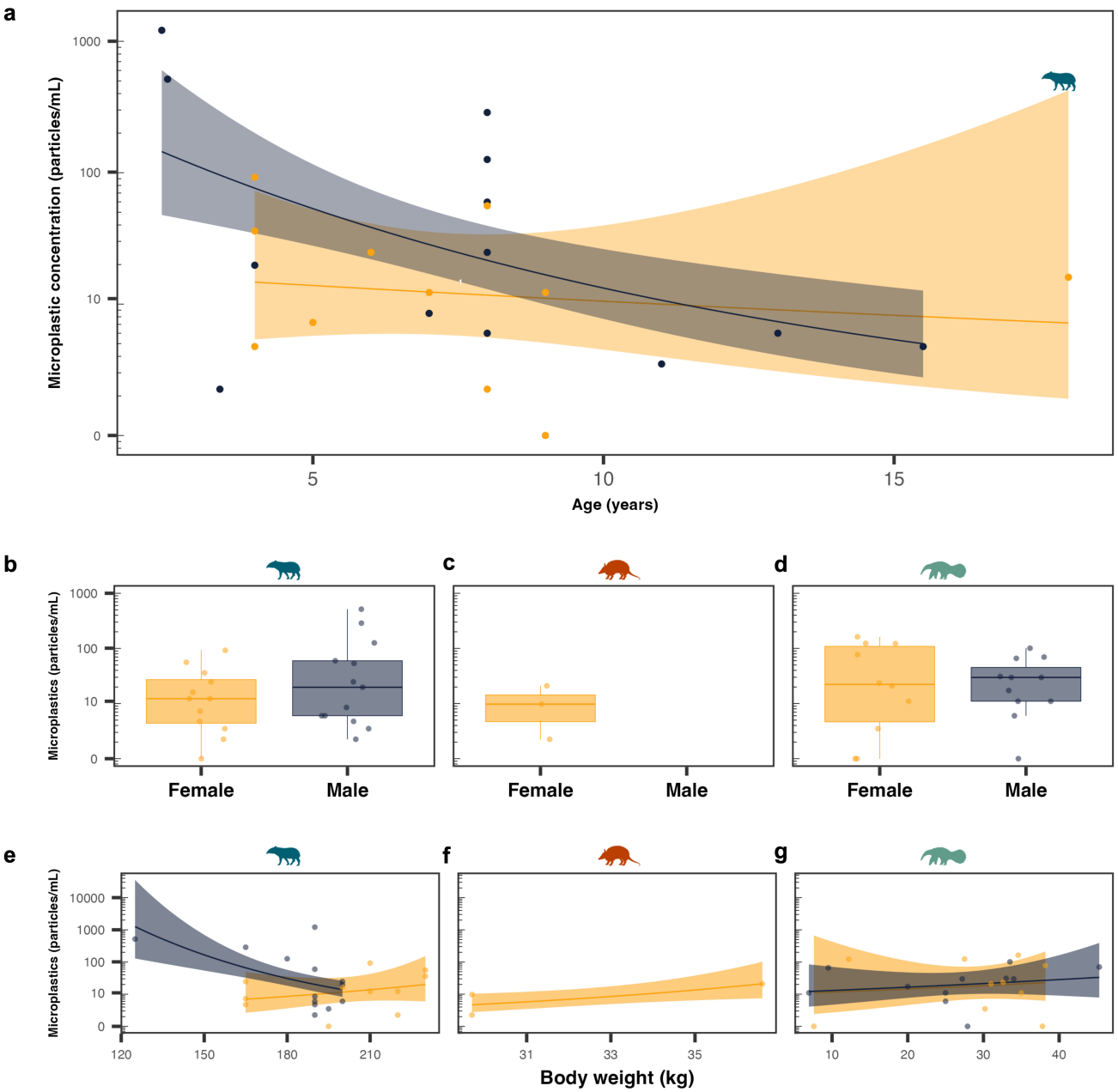
Correspondence and requests for materials should be addressed to Marcia de Almeida Monteiro Melo Ferraz.

Peer review information *Nature* thanks the anonymous reviewers for their contribution to the peer review of this work. Peer reviewer reports are available.

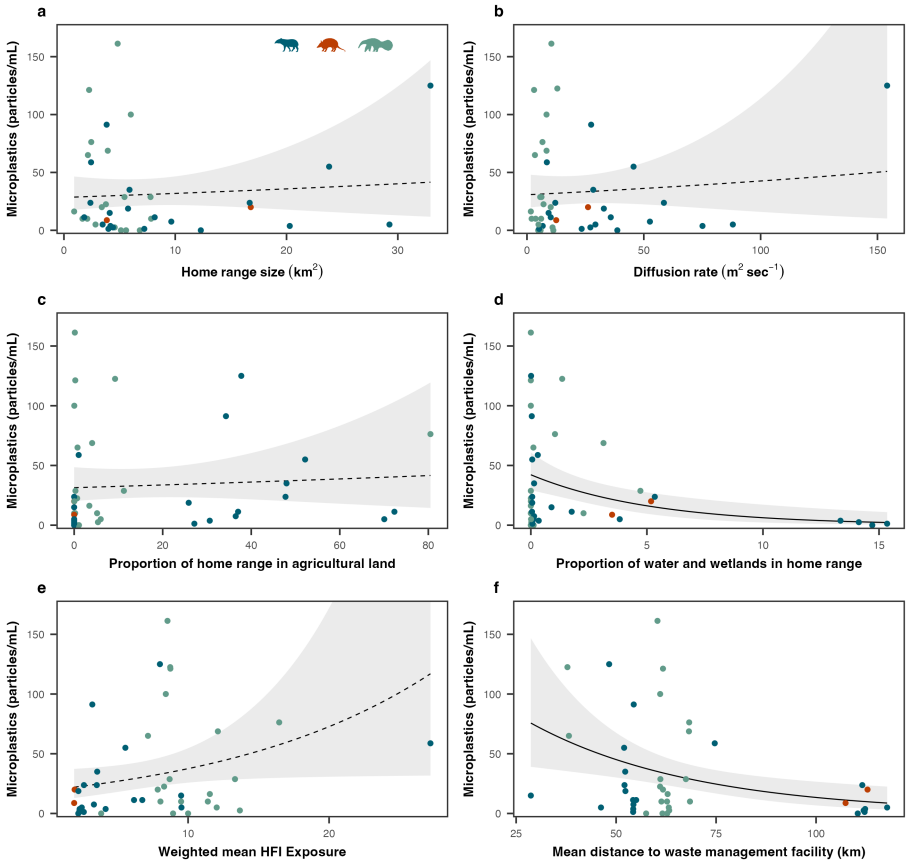
Reprints and permissions information is available at http://www.nature.com/reprints.



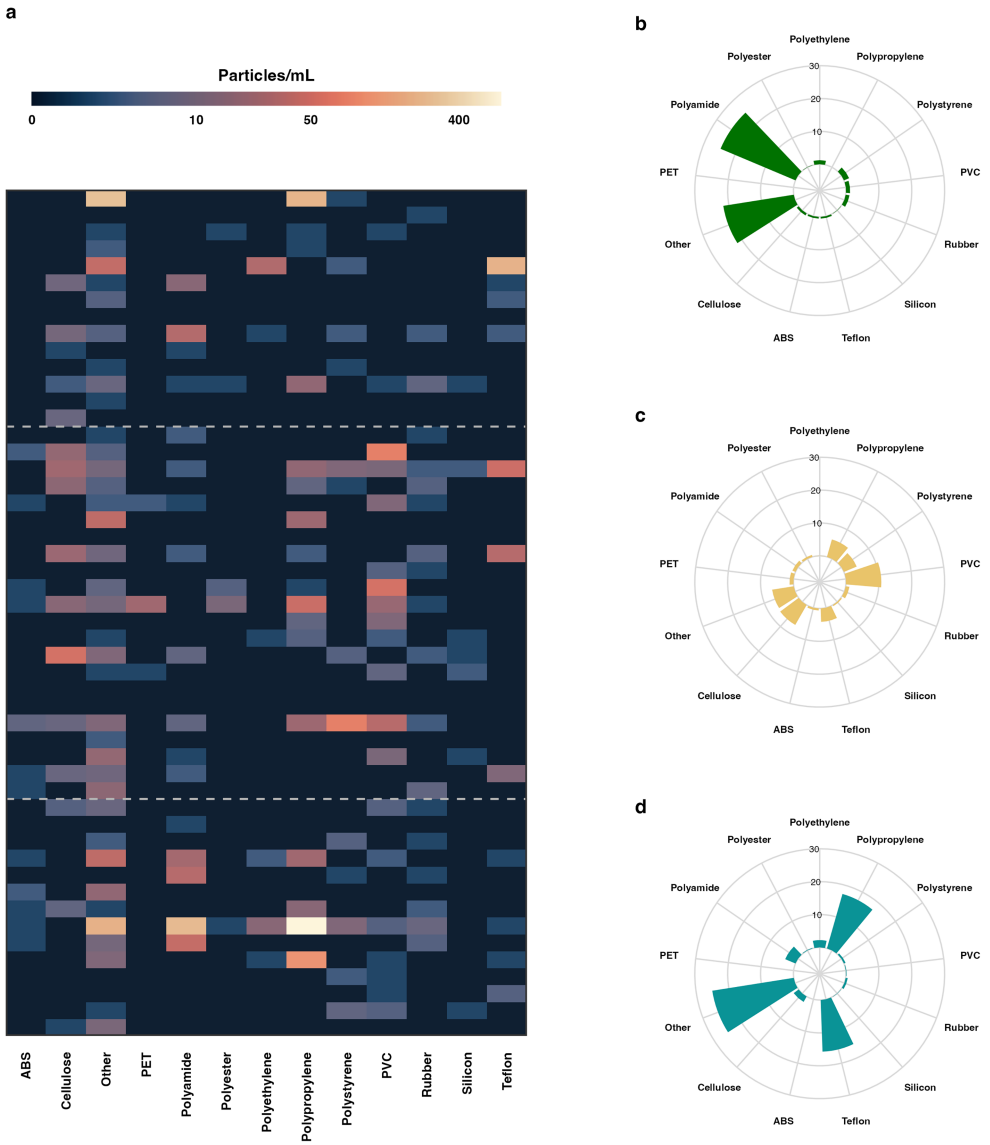
Extended Data Fig. 1 | Overview of the dataset with blood microplastic characterization across species. The radial bar plots show the mean concentrations (particles per ml) of the different plastic polymers within the blood samples of **a**, lowland tapirs ($n = 26$ animals) **b**, giant anteaters ($n = 21$ animals), and **c**, giant armadillos ($n = 3$ animals). The barplots in **d**, show the concentrations of the plastic particles in each animal. Histograms of the **e**, length and **f**, width of the individual particles are also shown ($n = 2,815$ particles). The average particle length was 10.2 µm (SD: 10.6, range: 2.0–167.2), and the width was 6.3 µm (SD: 5.2, range: 0.6–76.0). In panels **a**,**d**, polymers categorized as 'other' were those that occurred at low abundance, and included: Polyvinyl Butyralolyethyleneimine, Poly(butylene terephthalate), Polyvinylformal, Polyacetal, Polymethylpentene, Polyurethane, Polyethylene Glycol, amongst others. Data from giant armadillos are shown for visual comparison but were not included in the analyses presented in the main text. In **d**,**e**, Giant anteater image credit: Steven Traver via PhyloPic (CC0 1.0); tapir image credit: Christophe Mallet via PhyloPic (CC0 1.0); giant armadillo image credit: Steven Traver via PhyloPic (CC0 1.0).



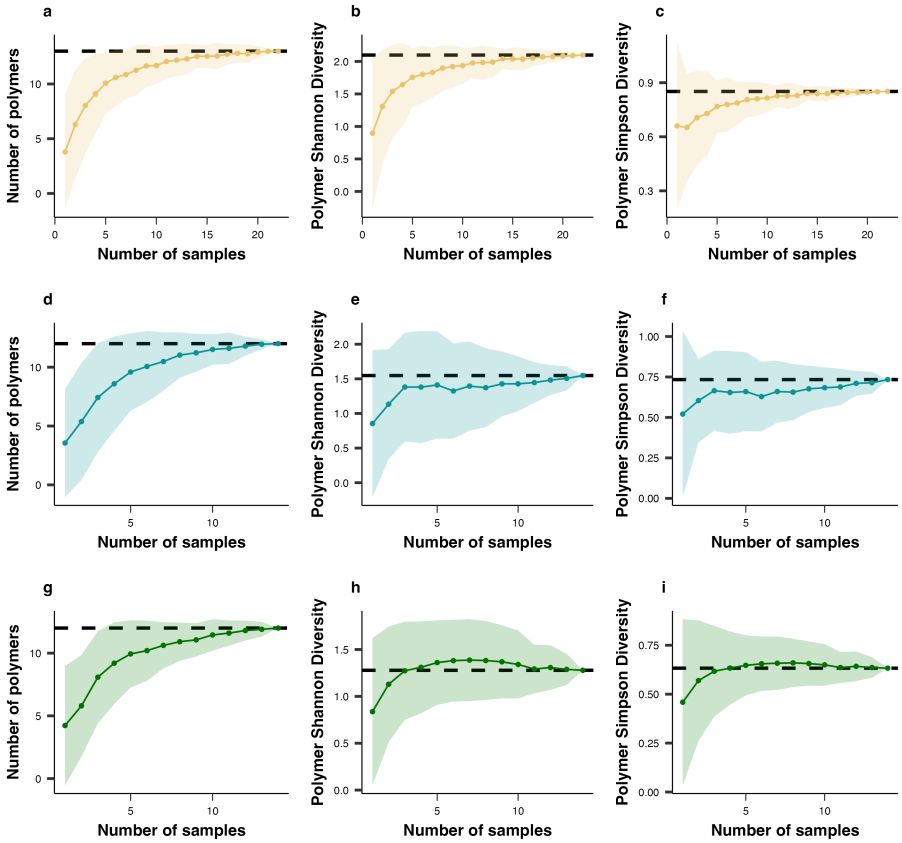
Extended Data Fig. 2 | Relationships between microplastic concentrations and biological variables. The scatter plot in **a**, shows the relationships between microplastic concentrations (particles per ml) and age for lowland tapirs ($n = 24$ animals). The boxplots compare microplastic concentrations (particles per ml) between females and males for the **b**, lowland tapirs ($n = 26$ animals; 12 females, 14 males) **c**, giant armadillos ($n = 3$ animals; all females), and **d**, giant anteaters ($n = 21$ animals; 10 females, 11 males). All boxplots depict centre line, median; box limits, 25th and 75th percentiles; whiskers, 1.5× interquartile range; points, individual animals. Scatter plots show the relationships between microplastic concentrations (particles per ml) and body weight (kg) for the **e**, lowland tapirs ($n = 24$ animals), **f**, giant armadillos ($n = 3$ animals), and **g**, giant anteaters ($n = 21$ animals). Lines in **a**),**e**,**f**,**g**, show the fitted population-level trend from a hierarchical generalised linear model (Tweedie distribution; log link) with species-specific random intercepts and slopes; shaded bands are 95% confidence intervals. *P*-values are based on two-sided tests, with no correction for multiple comparisons; a: $\beta = -0.26$, $t = -3.13$, $P = 0.0049$ (not robust to removal of the two youngest animals: $\beta = -0.16$, $t = -1.44$, $P = 0.17$); b: $\beta = 2.05$, $t = 3.36$, $P < 0.005$; d: $\beta = -0.49$, $t = -1.01$, $P = 0.327$; e: $\beta = -0.016$, $t = -1.10$, $P = 0.29$; g: $\beta = 0.012$, $t = 0.49$, $P = 0.63$. Coefficients are on the link scale. Data from giant armadillos (c,f; $\beta = 0.06$, $t = 0.62$, $P = 0.58$) are shown for visual comparison but were not included in the analyses presented in the main text. In **a**–**e**, Created in BioRender; Ferraz, M. https://BioRender.com/vp3npr1 (2026). Giant anteater image credit: Steven Traver via PhyloPic (CC0 1.0); tapir image credit: Christophe Mallet via PhyloPic (CC0 1.0); giant armadillo image credit: Steven Traver via PhyloPic (CC0 1.0).



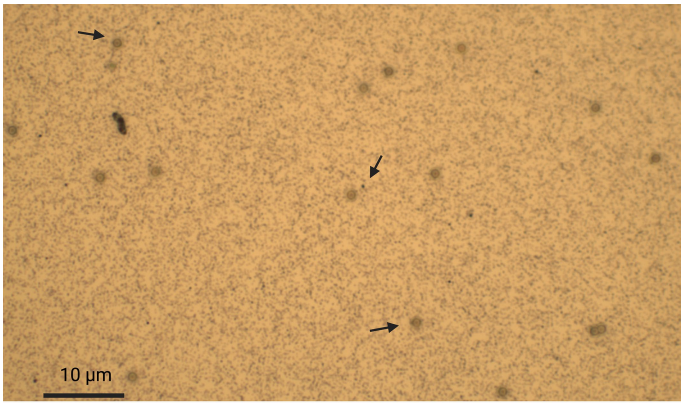
Extended Data Fig. 3 | Relationships between habitat use and microplastic concentrations in the 42 animals for which we had GPS tracking data. The scatter plots show the relationships between microplastic concentrations (particles per ml) and **a**, home-range size; **b**, diffusion rate; **c**, proportion of home range in agricultural land; **d**, proportion of home range in water and wetlands; **e**, weighted mean HFI exposure; and **f**, distance to the nearest waste management facility for all three species. In all panels, solid lines depict statistically significant relationships, whereas non-significant relationships are depicted with dashed lines. Lines in **a**,**b**,**c**,**d**,**e**,**f**, show the fitted population-level trend from a hierarchical generalised linear model (Tweedie distribution; log link) with species-specific random intercepts and slopes; shaded bands are 95% confidence intervals. *P*-values are based on two-sided tests, with no correction for multiple comparisons; a: $\beta = 0.0039$, $t = 1.49$, $P = 0.14$; b: $\beta = 0.037$, $t = 0.89$, $P = 0.38$; c: $\beta = 9.40 \times 10^{-4}$, $t = 1.20$, $P = 0.24$; d: $\beta = -0.17$, $t = -3.50$, $P = 0.0011$; e: $\beta = 0.061$, $t = 1.73$, $P = 0.092$; f: $\beta = -0.026$, $t = -2.73$, $P = 0.0096$. Coefficients are on the link scale. Data from giant armadillos are shown for visual comparison but were not included in the analyses presented in the main text. In **a**, giant anteater image credit: Steven Traver via PhyloPic (CC0 1.0); tapir image credit: Christophe Mallet via PhyloPic (CC0 1.0); giant armadillo image credit: Steven Traver via PhyloPic (CC0 1.0).



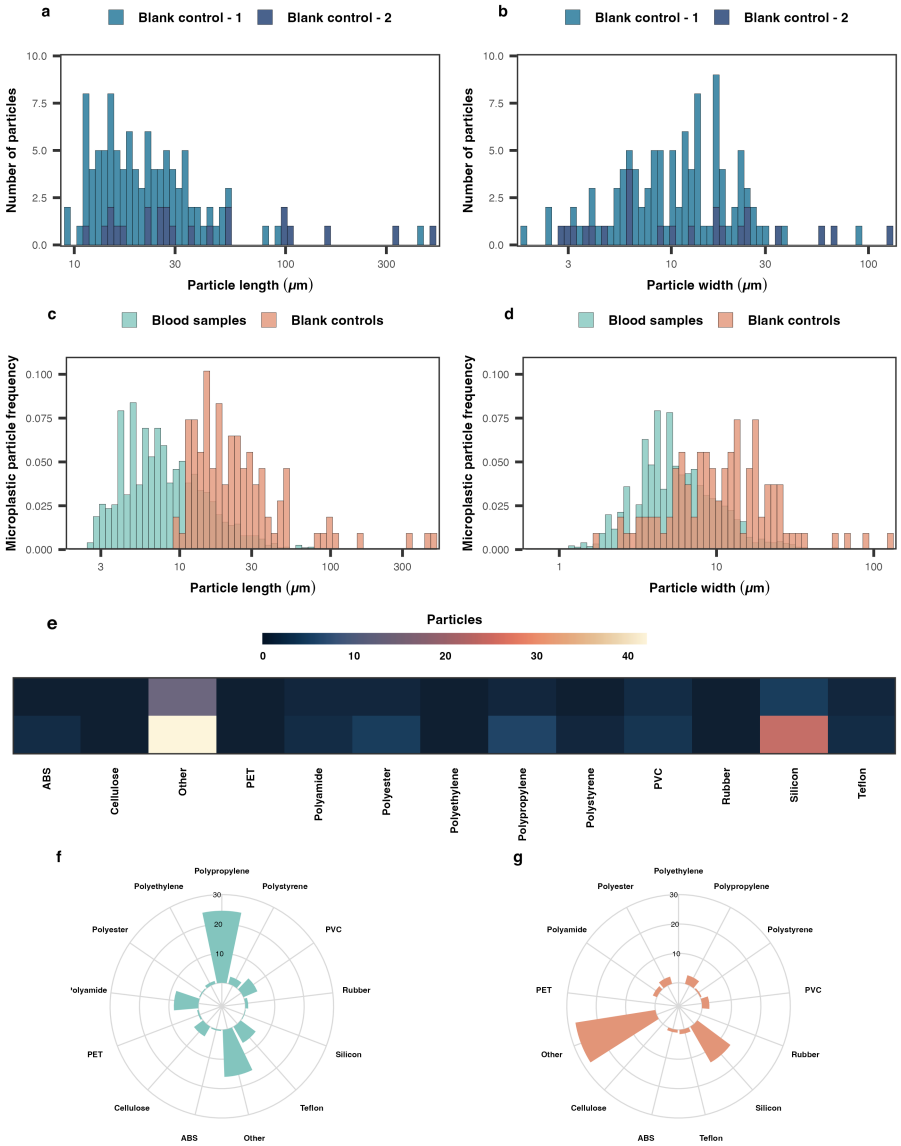
Extended Data Fig. 4 | Differences in plastic polymers between collection sites. Heatmap in **a**, depicting the concentration (particles per ml) of the analyzed microplastic polymers for data from the field sites at the Amazon deforestation frontier, the Cerrado agricultural mosaic, and the Pantanal cattle ranch. Each row in the heatmap corresponds to a unique blood sample. Rows are grouped by site and separated by dashed lines; the top lines are from the Pantanal cattle ranch (Baía das Pedras Ranch, Nhecolândia, Aquidauana, Mato Grosso do Sul), the middle lines from the Cerrado agricultural mosaic (between Nova Alvorada do Sul and Nova Andradina, and along the BR-267 and BR-262 highways, Mato Grosso do Sul), and the bottom lines from the Amazon deforestation frontier (Tanguro Farm, Querência, Mato Grosso). The radar bar plots show the mean concentrations (particles per ml) of the different plastic polymers within the blood samples of animals from the **b**, Amazon deforestation frontier site ($n = 14$ animals) **c**, Cerrado agricultural mosaic ($n = 22$ animals), and **d**, Pantanal cattle ranch ($n = 14$ animals). In all panels, polymers categorised as 'other' were those that occurred at low abundance, and included: Polyvinyl Butyralolyethyleneimine, Poly(butylene terephthalate), Polyvinylformal, Polyacetal, Polymethylpentene, Polyurethane, Polyethylene Glycol, amongst others. Pairwise site comparisons used a hierarchical generalised linear model (Tweedie distribution; log link) with species-specific random intercepts and slopes. *P*-values adjusted for multiple testing using the Benjamini-Hochberg procedure; Cerrado versus Pantanal PVC: $\beta = 3.54$, $t = 3.36$, adjusted $P = 0.037$; Amazon versus Cerrado polyamide: $\beta = 3.19$, $t = 3.47$, adjusted $P = 0.037$. No other pairwise polymer differences were detected. Overall concentrations did not differ across sites (generalized likelihood-ratio test, $\lambda = 3.39$, $P = 0.61$). All *P*-values are based on two-sided tests.



Extended Data Fig. 5 | Sensitivity analysis on polymer profiles sampling sites. Scatterplots of the number of polymers identified in blood samples, as well as the Shannon and Simpson's diversity indices as a function of the sample size. The top row **a**–**c**, shows results for data from the agricultural mosaic in the Cerrado ($n = 22$ animals), the middle row **d**–**f**, the cattle ranch in the Pantanal ($n = 14$ animals), and the bottom row **g**–**i**, the Amazon deforestation frontier site ($n = 14$ animals). In all panels, the dashed line represents the value estimated from the full dataset, the coloured lines connecting the points are included as a visual aid, and the shaded areas represent the 95% confidence intervals. Note how all curves exhibit saturating behaviour, however, clear convergence was limited for the data from the Pantanal site, and results from that site should be interpreted with caution.



Extended Data Fig. 6 | Polystyrene beads remain intact after the digestion process. Representative image of 1.1 µm polystyrene beads after the complete digestion and filtration workflow. Black arrows indicate polystyrene beads. Scale bar, 10 µm. The digestion test was repeated three times independently with similar results. Created in BioRender; Ferraz, M. https://BioRender.com/o4creek (2026).



Extended Data Fig. 7 | Size and polymer distributions of the plastic particles in the blank controls relative to the blood samples. Histograms of the **a**, length and **b**, width of the individual particles are shown ($n = 108$ particles). The two blank controls were processed in parallel with each of the two sample batches to monitor background contamination. The average particle length in the controls was 38.4 µm (SD: 69.6, range: 9.3–497.4), and the width was 14.9 µm (SD: 16.4, range: 1.7–124.0). Panels **c**,**d**, show the size distributions of the particles in the blank controls contrasted against the blood samples ($n = 2,815$ particles). The heatmap in **e**, shows the particle counts for the polymers in each of the two controls, while the radial bar plots show the polymer distributions in the **f**, blood samples, and **g**, controls.

Extended Data Table 1 | Number of individuals analyzed for each species, site, age class, sex and average weight (kg)

Species	Site	Age class	Number of individuals	Average weight (kg)
Myrmecophaga tridactyla	Cerrado Agricultural Mosaic	Cub	2 Females 2 Males	9.1
	Cerrado Agricultural Mosaic	Young	4 Males	24.3
	Cerrado Agricultural Mosaic	Adult	8 Females 5 Males	34.0
Priodontes maximus	Pantanal Ranch	Young	1 Female	29.7
	Pantanal Ranch	Adult	2 Females[a]	31.5
Tapirus terrestris	Pantanal Ranch	Young	1 Female 2 Males	157.5
	Pantanal Ranch	Adult	4 Females 4 Males	174.2
	Amazon Deforestation Frontier	Young	1 Male	190.0
	Amazon Deforestation Frontier	Adult	7 Females 6 Males	206.2
	Cerrado Agricultural Mosaic	Adult	1 Male	190.0

[a]measurements were performed in 2021 and 2022.

Extended Data Table 2 | Robustness of associations between blood microplastic concentrations and land-use exposure metrics across species subsets

	$\hat{\beta}$	*SE*	*t*	*P*
Maximum HFI				
All species (*n* = 42)	0.068	0.024	2.77	0.0084
Tapir and Giant anteater (*n* = 40)	0.07	0.026	2.66	0.011
Tapir only (*n* = 20)	0.056	0.029	1.93	0.069
Distance to Development				
All species (*n* = 42)	-0.024	0.01	-2.45	0.019
Tapir and Giant anteater (*n* = 40)	-0.032	0.01	-2.93	0.0057
Tapir only (*n* = 20)	-0.029	0.01	-2.86	0.01
Distance to Waste Management Facility				
All species (*n* = 42)	-0.024	0.0084	-2.84	0.0071
Tapir and Giant anteater (*n* = 40)	-0.026	0.0095	-2.73	0.0096
Tapir only (*n* = 20)	-0.024	0.0094	-2.55	0.02

$\hat{\beta}$: estimated regression coefficient on the link scale; SE: standard error; *t*: *t*-statistic; *P*: *P*-value. All *P*-values are based on two-sided tests from a hierarchical generalised linear model (Tweedie distribution; log link) with species-specific random intercepts and slopes, without any adjustments for multiple comparisons. Note: all of the tapir samples were processed in the same batch under identical laboratory conditions. The within species results thus also provide confirmation that trends are unlikely to have been influenced by sample contamination.

Extended Data Table 3 | Sensitivity of associations between blood microplastic concentrations and land-use exposure metrics to high-leverage observations

	$\hat{\beta}$	*SE*	*t*	*P*
Maximum HFI				
Below 95th quantile (*n* = 39)	0.11	0.038	2.77	0.0087
Below 90th quantile (*n* = 35)	0.18	0.046	2.53	0.016
Distance to Development				
Below 95th quantile (*n* = 39)	-0.031	0.012	-2.62	0.013
Below 90th quantile (*n* = 37)	-0.025	0.015	-1.68	0.1
Distance to Waste Management Facility				
Below 95th quantile (*n* = 39)	-0.024	0.01	-2.34	0.025
Below 90th quantile (*n* = 37)	-0.018	0.012	-1.52	0.14

$\hat{\beta}$: estimated regression coefficient on the link scale; SE: standard error; *t*: *t*-statistic; *P*: *P*-value. All *P*-values are based on two-sided tests from a hierarchical generalised linear model (Tweedie distribution; log link) with species-specific random intercepts and slopes, without any adjustments for multiple comparisons.

nature portfolio

Corresponding author(s): Marcia de Almeida Monteiro Melo Ferraz

Last updated by author(s): Sep 25, 2026

Reporting Summary

Nature Portfolio wishes to improve the reproducibility of the work that we publish. This form provides structure for consistency and transparency in reporting. For further information on Nature Portfolio policies, see our Editorial Policies and the Editorial Policy Checklist.

Statistics

For all statistical analyses, confirm that the following items are present in the figure legend, table legend, main text, or Methods section.

n/a	Confirmed
☐	☒ The exact sample size (*n*) for each experimental group/condition, given as a discrete number and unit of measurement
☐	☒ A statement on whether measurements were taken from distinct samples or whether the same sample was measured repeatedly
☐	☒ The statistical test(s) used AND whether they are one- or two-sided *Only common tests should be described solely by name; describe more complex techniques in the Methods section.*
☐	☒ A description of all covariates tested
☐	☒ A description of any assumptions or corrections, such as tests of normality and adjustment for multiple comparisons
☐	☒ A full description of the statistical parameters including central tendency (e.g. means) or other basic estimates (e.g. regression coefficient) AND variation (e.g. standard deviation) or associated estimates of uncertainty (e.g. confidence intervals)
☐	☒ For null hypothesis testing, the test statistic (e.g. *F*, *t*, *r*) with confidence intervals, effect sizes, degrees of freedom and *P* value noted *Give P values as exact values whenever suitable.*
☒	☐ For Bayesian analysis, information on the choice of priors and Markov chain Monte Carlo settings
☐	☒ For hierarchical and complex designs, identification of the appropriate level for tests and full reporting of outcomes
☒	☐ Estimates of effect sizes (e.g. Cohen's *d*, Pearson's *r*), indicating how they were calculated

Our web collection on statistics for biologists contains articles on many of the points above.

Software and code

Policy information about availability of computer code

Data collection	GPS location data were collected with Telonics GPS collars (TGW SOB and GPS IRIDIUM models; lowland tapirs) and Telonics GPS harnesses (giant anteaters). Confocal Raman data were acquired on a WITec alpha300 R microscope (UHTS 300 spectrometer, 532 nm laser) operated with WITec Control FIVE (WITec Suite FIVE, v5). Particles were detected and located with WITec ParticleScout, spectra were processed with WITec Project FIVE (v5) for background and cosmic-ray correction, and spectral matching was performed with WITec TrueMatch, both part of the WITec Suite FIVE.
Data analysis	All analyses were conducted in R v4.3.3 using ctmm v1.2.1, mgcv v1.9-1, weights v1.0.4, terra v1.8-54, sf v1.0-21, lwgeom v0.2-14, fields v16.3, tmap v4.0.0.9000, rnaturalearth v1.0.1, geobr v1.9.1, ggplot2 v3.5.2, ggspatial v1.1.9, tidyterra v0.7.0, rphylopic v1.5.0, fmsb v0.7.6 and gridExtra v2.3. All custom code is publicly available on figshare (https://doi.org/10.6084/m9.figshare.34001445.v1) and GitHub (https://github.com/QuantitativeEcologyLab/microplastics_brazil).

For manuscripts utilizing custom algorithms or software that are central to the research but not yet described in published literature, software must be made available to editors and reviewers. We strongly encourage code deposition in a community repository (e.g. GitHub). See the Nature Portfolio guidelines for submitting code & software for further information.

Data

Policy information about availability of data

All manuscripts must include a data availability statement. This statement should provide the following information, where applicable:

- Accession codes, unique identifiers, or web links for publicly available datasets
- A description of any restrictions on data availability
- For clinical datasets or third party data, please ensure that the statement adheres to our policy

The blood microplastics data (particle-level measurements, polymer identifications and per individual summaries underlying Figs. 1 and 2, Extended Data Figs. 1–2 and 4–7 and Extended Data Tables 1–3), raw GPS tracking data, and the per-individual movement and land-use summaries (underlying Fig. 2 and Extended Data Fig. 3) are available at https://doi.org/10.6084/m9.figshare.34001445 and on GitHub (https://github.com/QuantitativeEcologyLab/microplastics_brazil). Source data are provided with this paper. This study also used the following publicly available datasets: the 100 m Human Footprint Index (Gassert et al.[38]; https://source.coop/repositories/vizzuality/hfp-100/description); the Wildlife Conservation Society 300 m Human Footprint rasters for 2001 and 2020 (https://wcshumanfootprint.org/data-access); MapBiomas Brazil Collection 10 land use and land cover maps (https://brasil.mapbiomas.org/en/map/colecao-10/, downloads at https://brasil.mapbiomas.org/en/downloads/); waste management facility locations from the Waste Methane Assessment Platform (WasteMAP) v1.5.0, developed by RMI and Clean Air Task Force (https://wastemap.earth (https://wastemap.earth/)); and Natural Earth (https://www.naturalearthdata.com (https://www.naturalearthdata.com/)) and geobr [ref 68] basemap data. Raman spectra were matched against the SLoPP library (ref. 61; openly available) and the S.T. Japan commercial spectral database (S.T. Japan Europe GmbH), which is available under licence from the vendor.

Research involving human participants, their data, or biological material

Policy information about studies with human participants or human data. See also policy information about sex, gender (identity/presentation), and sexual orientation and race, ethnicity and racism.

Reporting on sex and gender	NA
Reporting on race, ethnicity, or other socially relevant groupings	NA
Population characteristics	NA
Recruitment	NA
Ethics oversight	NA

Note that full information on the approval of the study protocol must also be provided in the manuscript.

Field-specific reporting

Please select the one below that is the best fit for your research. If you are not sure, read the appropriate sections before making your selection.

☐ Life sciences ☐ Behavioural & social sciences ☒ Ecological, evolutionary & environmental sciences

For a reference copy of the document with all sections, see nature.com/documents/nr-reporting-summary-flat.pdf

Ecological, evolutionary & environmental sciences study design

All studies must disclose on these points even when the disclosure is negative.

Study description	Observational field study examining associations between anthropogenic land-use change and systemic microplastic burdens in free-ranging terrestrial mammals. Hierarchical design with individual animals as the unit of analysis, nested within species, across three sites spanning a gradient of human disturbance in Brazil.
Research sample	GPS-collared lowland tapirs (Tapirus terrestris; n=26, mixed sex and age) and giant anteaters (Myrmecophaga tridactyla; n=21, mixed sex and age) sampled at three sites in Brazil representing distinct land-use contexts: an agricultural mosaic in the Cerrado, the Arc of Deforestation in the Amazon, and a relatively undisturbed cattle ranch in the Pantanal. Species were selected based on existing long-term monitoring programs and their ecological diversity across dietary guilds.
Sampling strategy	No formal sample size calculation was performed. Sample sizes were determined by capture feasibility given the logistical constraints of live-capturing large, threatened, free-ranging mammals under national ethical permits. All animals safely captured during the study period were included.
Data collection	Blood samples and GPS tracking data were collected by trained field teams during animal captures conducted between February 2021 and November 2022. Microplastic analysis was performed by laboratory staff using confocal Raman spectroscopy.

Timing and spatial scale	February 2021 to November 2022. Three discrete field sites in Brazil covering home ranges of individual animals estimated at the 95% AKDE isopleth.
Data exclusions	Seven blood samples lacked sufficient GPS tracking data for inclusion in habitat use analyses and were excluded from the regression models but retained in descriptive analyses. GPS locations identified as outliers (n=16,656, 3.55% of total) were removed prior to movement modelling using error-informed distance filtering. Exclusion criteria were pre-established.
Reproducibility	All analytical scripts and data are publicly available at the GitHub repository. The movement modelling and statistical analyses are fully reproducible from the archived data and scripts.
Randomization	NA
Blinding	NA

Did the study involve field work? ☒ Yes ☐ No

Field work, collection and transport

Field conditions	Three sites in Brazil with distinct climatic conditions. The Cerrado agricultural mosaic experiences marked precipitation seasonality with ~70% of annual rainfall between November and March. The Pantanal site experiences average annual temperatures of 25°C and annual rainfall of 1,185 mm with seasonal flooding. The Amazon site experiences a prolonged dry season (May–September) with annual rainfall of 1,700–2,200 mm.
Location	Three sites in Brazil. Cerrado agricultural mosaic: -21.99°, -53.83° (Nova Alvorada do Sul/Nova Andradina, Mato Grosso do Sul). Pantanal cattle ranch: -19.33°, -55.72° (Baía das Pedras Ranch, Nhecolândia, Mato Grosso do Sul). Amazon deforestation frontier: Tanguro Farm, Querência, Mato Grosso (-12.47°, -52.38° approximately).
Access & import/export	All animal captures and sampling procedures were authorized by the Brazilian Ministry of the Environment (MMA) and Instituto Chico Mendes de Conservação da Biodiversidade (ICMBio) under license numbers 14603-25 (lowland tapirs), 53798-18 (giant anteaters), and 27587-1 (giant armadillos). Blood samples were transported and processed in compliance with Brazilian national regulations. Field sites were accessed with landowner permission.
Disturbance	Animals were captured using established protocols designed to minimize stress and handling time. Chemical immobilization was performed under veterinary oversight. All animals were released at their capture sites following recovery. GPS collars were deployed as part of ongoing long-term monitoring programs and were retrieved or programmed to drop off at the end of the operational life.

Reporting for specific materials, systems and methods

We require information from authors about some types of materials, experimental systems and methods used in many studies. Here, indicate whether each material, system or method listed is relevant to your study. If you are not sure if a list item applies to your research, read the appropriate section before selecting a response.

Materials & experimental systems

n/a	Involved in the study
☒	☐ Antibodies
☒	☐ Eukaryotic cell lines
☒	☐ Palaeontology and archaeology
☐	☒ Animals and other organisms
☒	☐ Clinical data
☒	☐ Dual use research of concern
☒	☐ Plants

Methods

n/a	Involved in the study
☒	☐ ChIP-seq
☒	☐ Flow cytometry
☒	☐ MRI-based neuroimaging

Animals and other research organisms

Policy information about studies involving animals; ARRIVE guidelines recommended for reporting animal research, and Sex and Gender in Research

Laboratory animals	This study did not involve laboratory animals.
Wild animals	Free-ranging lowland tapirs (Tapirus terrestris; n = 26; 12 females, 14 males; 4 young and 22 adults; estimated ages 2.4–18 years for the 24 individuals with age estimates), giant anteaters (Myrmecophaga tridactyla; n = 21; 10 females, 11 males; 4 cubs, 4 young and 13 adults) and giant armadillos (Priodontes maximus; n = 3; all females; 1 young and 2 adults) were captured in the field using the species-appropriate methods described in the Methods. Age classes and sex by site are given in Extended Data Table 1. Blood samples were collected under chemical immobilization, and all animals were released at their capture sites after recovery. No

	animals were killed or kept in captivity as part of this study. GPS collars were deployed for ongoing telemetry monitoring as part of long-term conservation programmes.
Reporting on sex	Sex was recorded for all individuals and is reported in Extended Data Table 1. Sex-based analyses were conducted and are reported in the supplementary text and Extended Data Fig. 2. Findings apply to both sexes; male tapirs showed significantly higher microplastic concentrations than females, but no significant sex difference was found in giant anteaters. Sex was determined by physical examination during capture.
Field-collected samples	No animals were housed or maintained under laboratory conditions; photoperiod and end-of-experiment protocols are therefore not applicable. All animals were sampled once at capture (two giant armadillos were sampled at two time points) and released at their capture sites following recovery from anaesthesia. Blood was collected by venipuncture into pre-cleaned glass tubes without preservatives, sealed with pre-cleaned aluminium foil and a metal cap. Lowland tapirs: ~10 mL collected within 20 min of immobilization; kept shaded at ambient temperature (no field refrigeration at the remote sites) and frozen at −20 °C on return to base camp within 5–6 h. Giant anteaters and giant armadillos: ~5 mL collected ~20 min after induction; kept at 4 °C on site and frozen at −20 °C within 12–24 h. All samples were stored at −20 °C for ~1–22 months (collection Feb 2021–Nov 2022) until digestion in Dec 2022; isolated particles on filter membranes were stored in pre-cleaned glass Petri dishes and analysed by Raman spectroscopy between Jan and Dec 2023. Full details are provided in the Methods.
Ethics oversight	All capture and sampling procedures were approved by the Brazilian Ministry of the Environment (MMA) and Instituto Chico Mendes de Conservação da Biodiversidade (ICMBio) under license numbers 14603-25 (lowland tapirs), 53798-18 (giant anteaters), and 27587-1 (giant armadillos).

Note that full information on the approval of the study protocol must also be provided in the manuscript.

Plants

Seed stocks	NA
Novel plant genotypes	NA
Authentication	NA